DOI: 10.1534/genetics.110.120683

Different Aneuploidies Arise From the Same Bridge-Induced Chromosomal Translocation Event in *Saccharomyces cerevisiae*

Beatrice Rossi, Pawan Noel and Carlo V. Bruschi[1]

International Centre for Genetic Engineering and Biotechnology, Yeast Molecular Genetics Laboratory, I-34149 Trieste, Italy

Manuscript received July 9, 2010
Accepted for publication August 6, 2010

ABSTRACT

Chromosome translocations are gross chromosomal rearrangements that have often been associated with cancer development in mammalian cells. The feasibility of drastically reshaping the genome with a single translocation event also gives this molecular event a powerful capacity to drive evolution. Despite these implications and their role in genome instability, very little is known about the molecular mechanisms that promote and accompany these events. Here, at the molecular level, we describe 10 morphologically and physiologically different translocants ensuing from the induction of the same bridge-induced translocation (BIT) event in the budding yeast *Saccharomyces cerevisiae*. We have demonstrated that, despite their common origin from the integration of the same linear DNA construct, all 10 translocation mutant strains have different phenotypes and the ability to sporulate and regulate gene expression and morphology. We also provide insights into how heterogeneous phenotypic variations originate from the same initial genomic event. Here we show eight different ways in which yeast cells have dealt with a single initial event inducing translocation. Our results are in agreement with the formation of complex rearrangements and abnormal karyotypes described in many leukemia patients, thus confirming the modellistic value of the yeast BIT system for mammalian cells.

TRANSLOCATIONS between nonhomologous chromosomes are some of the most severe genomic aberrations, which in higher eukaryotes often lead to malignant transformation. In humans, they have been associated with hematological cancers such as myelogenous leukemia but also with lymphomas, solid tumors, and recently, with mesenchymal and epithelial cancers (Dalla-Favera *et al.* 1982; Nowell 1988; Rowley 2001, 2008; Taki and Taniwaki 2006; Gasparini *et al.* 2007; Nickoloff 2008). In the past few decades, molecular and cytological studies have demonstrated that different chromosomal abnormalities such as aneuploidy can be associated with a translocation event in cancer cells. For example, acute transformation of leukemia patients is often associated with the duplication of the Philadelphia chromosome, trisomy 8 and isochromosome 17q, or other complex chromosomal rearrangements (Muehleck *et al.* 1984; Bernstein 1988; De Braekeleer 2007). Furthermore, unbalanced translocations can be detected in older leukemia patients. Karyotypic analyses have revealed that unbalanced translocations can advance into further rearrangements of the chromosomes involved in the translocations. This can give rise to complex and abnormal karyotypes characterized by monosomy, disomy, and trisomy for different segments of the translocation participant chromosomes (Pedersen *et al.* 2000).

Many molecular studies have been performed to better understand the formation of such severe chromosomal aberrations (Kanaar *et al.* 1998; Delneri *et al.* 2003; Aylon and Kupiec 2004; Egli *et al.* 2004; Motegi *et al.* 2006; Weinstock *et al.* 2006; Motegi and Myung 2007). Nevertheless, very little is known about the mechanisms by which chromosome translocations and secondary rearrangements arising from these events occur. The occurrence of two or more double-strand breaks (DSB) and an inappropriate use of the recombination machinery of the cells are supposed to be some of the main ways in which a DNA translocation is promoted (Rowley 2001, 2008; Agarwal *et al.* 2006). In humans, defects in many DSB repair mechanisms such as non-allelic homologous recombination, nonhomologous end-joining, and fork stalling and template switching (FoSTeS) have been reported to be involved in translocation formation (Gu *et al.* 2008). In yeast cells, single-strand annealing and break-induced replication (BIR) pathways have been shown to be involved in the formation of chromosome rearrangements and translocations (Bosco and Haber 1998; Haber 2006).

Recently, our group described a method that allows the generation and subsequent selection of chromo-

Supporting information is available online at http://www.genetics.org/cgi/content/full/genetics.110.120683/DC1.

[1]*Corresponding author:* ICGEB-Yeast Molecular Genetics Laboratory, AREA Science Park-W, Padriciano 99, I-34149 Trieste, Italy.
E-mail: bruschi@icgeb.org

somal translocations between any two chromosomal loci in diploid yeast strains. This was done by transformation of whole yeast cells with a linear DNA construct, carrying the KAN^R selectable marker flanked by DNA sequences homologous to two different chromosomal loci (Tosato *et al.* 2005, 2009; Nikitin *et al.* 2008).

We used this method to investigate the multiple molecular mechanisms and pathways that might be involved during a translocation event in *Saccharomyces cerevisiae*. To this end, we generated a collection of 10 different mutant strains harboring a translocation between chromosomes XVI and IX (Figure 1), followed by their comparative molecular and physiological analyses. Results obtained from our experiments suggest that the induction of the same chromosomal translocation can lead to a wide variety of secondary chromosomal rearrangements, generating aneuploidy derived from partial or complete chromosome duplication or loss of genetic material.

Physiological analyses also revealed that the 10 translocants obtained with the bridge-induced translocation (BIT) system in this work have different mutant phenotypes, which are analogous to the high variation of phenotypes characteristic of cancer cells. We demonstrated that these mutant strains exhibit altered behavior and fitness in different carbon sources for growth, different sporulation efficiencies, and ability to flocculate. Expression analyses also show that they exhibit different expression profiles of various genes located along the translocated chromosome or involved in cellular processes such as apoptosis, cell cycle regulation, and oxidative stress response. Overall, our work shows that the single integration of a linear DNA cassette with homology on two different chromosomes not only can generate a translocation, but also might be responsible for other complex chromosomal rearrangements. Such complex genomic rearrangements seen in yeast may play a role as key evolutionary forces, reshaping and remodeling genomes, followed by selection and adaptation into specialized cells or even neoplastic transformation, as observed in mammalian cancer cells.

MATERIALS AND METHODS

Strains: The diploid *S. cerevisiae* strain San1 (Waghmare *et al.* 2003) was used as the recipient strain to induce the translocation between chromosomes XVI and IX. San1 was also used as the control strain throughout this work.

The SUSU translocants are all derivatives of San1 and were obtained using the BIT system (Tosato *et al.* 2005). The BIT cassette was amplified using the primers Fw(XVI) and Rev(IX) reported in the supporting information, Table S1A. Transformants were selected as kanamycin-resistant (Kan^R) strains, and the presence of the translocation between the *SSU1* and *SUC2* loci was monitored by PCR and Southern blot analysis. The two diploid mutant strains San1-*DBP1/dbp1::KANMX4* and San1-*GUT2/gut2::KANMX4* used in CHEF experiments are both derivatives of San1, and they were obtained using the standard PCR-based gene knockout technique. ΔFDBP1 (forward) and RKANDBP1 (reverse) primers were used for *DBP1* deletion cassette amplification, and GUT2ΔFw (forward) and GUT2ΔrevNEW (reverse) for *GUT2* deletion cassette amplification (Table S1C). Primers described in Table S1C were used to confirm the deletion in the transformants by PCR using genomic DNA. Strains I-2 and I-6 are derivatives of San1 carrying the *KANMX4* insertion in chromosome XVI at the translocation breakpoint. Strains I-11 and I-17 carry the same on chromosome IX. Primers used to amplify PCR-based integration cassettes for chromosome XVI and IX are reported in Table S1A, Table S1B, and Table S1C.

Growth conditions: All *S. cerevisiae* strains were grown at 30° in rich liquid or solid medium (YPD; Difco, Detroit). Geneticin G418 was added to select transformants and to grow the SUSU translocants (final concentration 200 μg/ml; Gibco, Rockville, MD). Raffinose [2% w/v, yeast extract, peptone, raffinose (YPR)] and glycerol (2% w/v, YPG) media were used to test the growth rate of the translocants. SPIII and SPII media, supplemented with amino acids, were used for sporulation tests (Kaiser *et al.* 1994).

The standard growth conditions to prepare samples for RT–PCR were as follows: cells were cultured in 100-ml baffled flasks with 10 ml medium in a shaking incubator at 30° and at 160 rpm. After 18 hr of preculturing in YPD, the cells were washed with sterile water and inoculated (10^5 cells/ml) in 250-ml flasks containing 20 ml of fresh YPD medium. After 16 hr of growth, cells were centrifuged and then resuspended in 1 ml of water. A volume corresponding to 0.3–0.5 OD_{600} of this suspension was then transferred to a new 250-ml flask containing 15 ml of fresh YPD or YPR medium. Cultures were further incubated for an additional 3 hr and then harvested for total RNA extraction.

Sporulation efficiency: The sporulation efficiency of all SUSU translocants grown in sporulation medium for 4–5 days was calculated as the percentage of the four-spored asci among the total number of cells counted under the microscope and compared with the San1 sporulation efficiency considered as 100%.

Microscopy: *DAPI staining:* A single isolated colony was grown in liquid rich medium at 30°. After 16, 40, or 72 hr growth, 1 ml of the culture was harvested and cells were stained with DAPI as described (Nikitin *et al.* 2008). A Leica DMLB fluorescence microscope was used to monitor DAPI-stained images of yeast cells.

FUN-1 staining: A single isolated colony was inoculated in a 100-ml flask containing 10 ml YPD medium and incubated at 30° for 18 hr to reach late log phase (10^7 cells/ml). A total of 200 μl of the cell suspension was then stained with FUN-1 dye diluted at an optimal concentration of 12.5 or 6.3 μM following the standard protocol suggested by the supplier (Molecular Probes, Eugene, OR). Cells were visualized under fluorescence using fluorescein and rhodamin filters. At least 300 cells were counted, and the ratio between metabolically inactive/dead cells (yellow) and metabolically active/alive cells [forming cylindrical red intravascular structures, or CIVSs (Millard *et al.* 1997)] was expressed as the percentage of cells that appeared yellow.

Plasmids and transformations: Plasmid pFA6-KanMX4 containing the *KANMX4* gene (Oka *et al.* 1981) was used as template for the amplification of the SUSU-BIT cassette. Transformation of *S. cerevisiae* was performed by the lithium acetate (LiAC) method following the EUROFAN protocol for PCR-based gene replacements (Wach *et al.* 1994) or by the spheroplast method following the instruction reported in Kaiser *et al.* (1994).

Molecular biology techniques: Standard recombinant DNA techniques were carried out essentially according to Sambrook *et al.* (1989). Genomic DNA purification kits and plasmid miniprep kits were obtained from Promega (Madison, WI).

Restriction enzymes and biochemicals, obtained from New England Biolabs (Beverly, MA), were used according to the manufacturer's instructions.

Semiquantitative RT–PCR analysis: Total RNA was isolated from cells using the SV Total RNA Isolation System (Promega) or the Total Quick RNA kit (Talent, Trieste, Italy). cDNA synthesis and semiquantitative PCR based on limiting the number of cycles (20–23 cycles) were performed as described (Nikitin *et al.* 2008).

RT–PCR results were quantified using a laser-scanning densitometry (UltroScan XL, Pharmacia LKB), and the intensity of each band (area) was calculated as the average of three different measures. The expression of the housekeeping gene *HSC82*, located on chromosome VIII, was used to normalize the data. Data presented in Figure 8 and Figure S4 are averages with standard errors from at least three independent determinations in which the final values are the expression level of each gene normalized with respect to its expression in the San1 control strain considered as a unit.

The primers used to amplify the different genes are described in Table S1A and Table S1B. *YCA1* and *HSC82* are located on chromosome XV, *CLB1* on chromosome VII, *CDC48* on chromosome IV, *GSH1* on chromosome X, and *VMR1* on chromosome VIII. All the other genes are located on chromosome IX or XVI (Table S3).

DNA copy-number determination: Determination of gene copy number of the genes located on the chromosomes IX and XVI in the different SUSU translocants was made by standard quantitative PCR using a limiting number of cycles (20–22 cycles). *ACT1* (on chromosome VI) was used as the control gene to normalize the data. To increase the accuracy of the experiment, *ACT1* was co-amplified together with the target gene in the same reaction tube. Values presented in Figure 3 are averages and standard errors from at least three independent determinations normalized with respect to *ACT1*, considered as a two-copy-number gene. A control experiment was carried out in which *ACT1* was amplified together with *VMR1*, a gene located on chromosome VIII, which is not involved in the translocation. Gel images presented are representative examples from at least four individual experiments.

The primers used to amplify the various genes are described in Table S1A and Table S1B. For *VMR1* and *SUC2* in the translocant chromosome, and for *GAL4* and *DAL4*, the same primers used in the RT–PCR experiments were utilized.

CHEF analyses: Agarose plug preparation and CHEF electrophoresis were performed as described (Tosato *et al.* 2005). Hybridization and detection were performed as for a standard Southern blot. Chromosome positions were calculated from bands of the membranes in Figure 2 by polynomial equation: (a) $y = -114.1\,X^2 - 7757\,X + 1{,}359{,}000$ was used to calculate the size of the SUSU9 aberrant chromosome; (b) $y = -1432\,X^2 + 179{,}631\,X - 300{,}727$ was used to calculate the size of the extra band in SUSU7; and (c) $y = -24{,}936.4\,X^2 + 495{,}490\,X - 1{,}305{,}740$ was used to calculate the size of the extra band in SUSU2.

Hybridization probes labeled using the polymerase chain reaction digoxygenin probe synthesis kit (Roche, Basel, Switzerland) were obtained from genomic DNA using primers described in Table S1A and Table S1B. For *GLN1*, *GLR1*, and *GAL4*, the same primers for both RT–PCR and gene copy-number experiments were used.

RESULTS

A new set of BIT translocants between chromosome XVI and IX: The previously described BIT system (Tosato *et al.* 2005) was used to generate a collection of 10 translocants between chromosomes XVI and IX of *S. cerevisiae*. The BIT construct used in this work harbors the *KANMX4* selectable marker flanked by two 65-bp sequences, one homologous to the terminator region of *SSU1* (that is also the promoter region for *GLR1*) and the other to the promoter region of *SUC2*, located on chromosomes XVI and IX, respectively (Figure 1). Both these loci harbor metabolic genes that are not involved in genome regulatory processes (Perlman *et al.* 1982; Taussig and Carlson 1983; Lutfiyya and Johnston 1996; Avram and Bakalinsky 1997; Perez-Ortin *et al.* 2002; Fleming and Pennings 2007). The aberrant chromosome generated by translocation between these two loci contains 374 kb of chromosome XVI and a 403-kb fragment of chromosome IX bridged together by the selectable marker KANMX4. The centromere of the translocant chromosome belongs to chromosome IX and is located in an acrocentric position. The resulting right arm of the aberrant chromosome corresponds to the short right arm of chromosome IX (Figure 1).

The PCR-amplified linear DNA cassette was used to transform the diploid yeast strain San1, following the selection of KAN^R transformants on G418-containing plates. We have used two different transformation techniques to induce BIT in San1 cells. A total of 104 transformants were obtained using the standard LiAc transformation, and a collection of 138 transformants were obtained using spheroplast transformation (Table S2). All transformants were analyzed by colony PCR to check the integration of the BIT construct at both target loci in the genome, using specific primers (see Figure 1). When the transformants showed integration at both loci, the presence of the translocation was confirmed by performing a bridge-PCR from genomic DNA and further validated by sequence analysis (data not shown; see Figure 1 for more details). Among a collection of 10 translocants obtained, 9 translocants were obtained by using the LiAc transformation technique and 1 translocant (*i.e.*, SUSU10) by using spheroplast transformation (Table S2). Our experiments showed that all the analyzed translocations are nonreciprocal (see the following paragraphs and Figures 2, 4, and 5). Furthermore, sequence analysis of the translocation breakpoints revealed no mismatches or mutations in all 10 mutant strains (data not shown).

One interesting observation was that the LiAc technique was ~10 times more efficient in inducing a BIT event in comparison to spheroplast transformation (8.6% translocation frequency with LiAc transformation, 0.7% translocation frequency with spheroplast transformation; Table S2). Moreover, we demonstrated that by using the spheroplast transformation protocol the frequency of ectopic integration was almost doubled in comparison to the LiAc transformation technique (63% *vs.* 37.5%; Table S2). This could be due to differential processing of the BIT cassette during its uptake into the nucleus or due to altered activation/

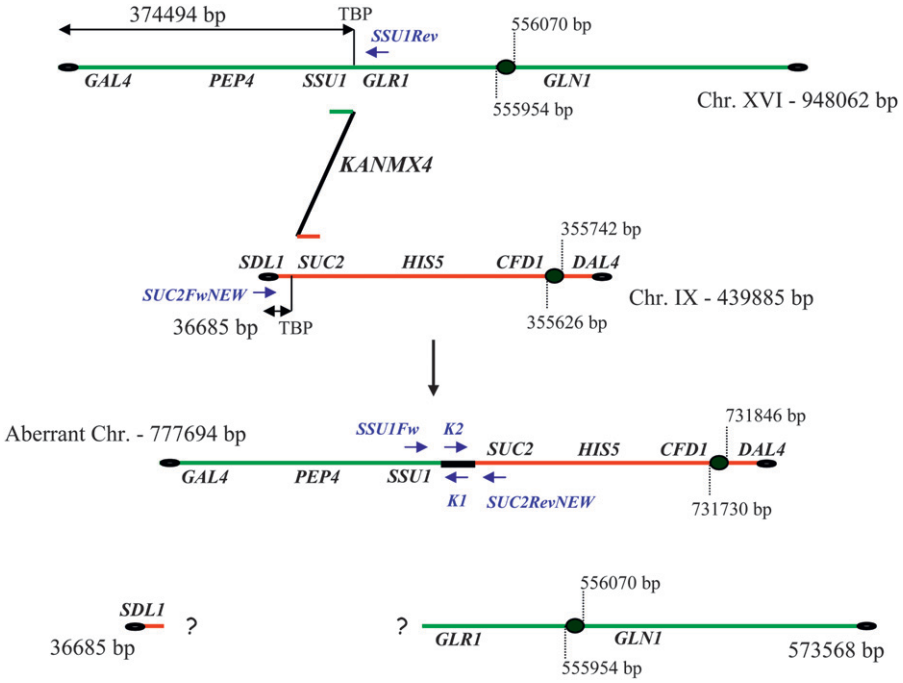

FIGURE 1.—Schematic of BIT between chromosomes XVI and IX. The 777,694-bp aberrant chromosome together with the two hypothetic fragments originating after a non-reciprocal BIT translocation are shown. Genes analyzed by Southern hybridization are reported along the chromosomes together with the primers used to test the integration of the BIT construct at the level of the two targeted loci. SSU1Fw and SUc2RevNEW primers were used to perform the bridge-PCR to validate the presence of the translocant chromosome (see RESULTS). TBP, translocation breakpoint.

stimulation of the DNA repair machinery by the two transformation procedures (HEALE *et al.* 1994).

Chromosomal pattern of the SUSU translocants: The chromosomal pattern of all the s**SU**1-**SU**c2 (*i.e.*, SUSU) translocants named SUSU1–SUSU10 was analyzed using pulsed-field gel electrophoresis PFGE followed by Southern blot analysis. These experiments further confirm that all translocations induced by transformation with a BIT cassette between two nonhomologous chromosomes are non-reciprocal (Figure 2).

Digoxygenin-labeled probes for *GAL4*, *PEP4*, *GLR1*, and *GLN1* were used to investigate the fate of the various parts of chromosome XVI; *SDL1*, *HIS5*, and *CFD1* probes were used to investigate the same for chromosome IX. A *KANMX4* probe was used to monitor the formation and occurrence of the aberrant chromosome.

Figure 2 (SDL1 panel) shows that the small acentric fragment of 36,685 bp (Figure 1), supposedly originating after the translocation, is lost or degraded. On the other hand, the 573,568-bp centromeric fragment of chromosome XVI (Figure 1) was not detected in all 10 translocants. These results, together with the gene copy-number data (the following paragraph and Figures 3, 4, and 5), suggest that this centromeric fragment was possibly copied via a BIR-like event during the integration of the BIT cassette at the *SSU1* locus. This mechanism has previously been proposed to be responsible for the generation of other translocants obtained with the BIT system between chromosomes V and VIII, XV, and VIII (TOSATO *et al.* 2005). Probes used against chromosome XVI revealed that SUSU2, SUSU7, and SUSU9 carry complex rearrangements of this chromosome (see Figure 5). In SUSU2, a fragment of chromosome XVI containing the *PEP4* and *GLR1* genes was rearranged elsewhere in the genome, leading to the formation of a novel chromosome (Figures 2 and 5). Using a polynomial equation to calculate chromosome size, this aberrant chromosome containing *PEP4* and *GLR1* was estimated to be ~1067 kb. In SUSU7, a large fragment of chromosome XVI encompassing the centromere was fused to another chromosomal fragment, giving rise to a bigger chromosome of ~1307 kb (see MATERIALS AND METHODS for calculations and Figures 2 and 5). Southern blot analyses revealed that in SUSU9 the aberrant chromosome containing the kanamycin resistance gene and the sequenced BIT junction between chromosome XVI and IX was larger than expected. This chromosome of ~1042 kb did not contain *GLR1*, *CFD1*, and *DAL4* (not shown) but harbored *GLN1*, as detected using specific probes. Thus, it does not contain the centromere of chromosome IX but it does contain that of chromosome XVI. Moreover, it seems that it lost a portion of chromosome XVI close to the translocation breakpoint. This different aberrant chromosome that is not a true translocant may have originated by a complex Fork stalling template switching-like mechanism during synthesis (see DISCUSSION and Figure 5). Hybridization with the KANMX4 probe demonstrated the presence of the expected 778-kb translocant chromosome in all the other SUSU mutant strains.

On the basis of the fact that the parental strain San1 is diploid, at least one copy of both wild-type chromosomes XVI and IX is also present in all mutant strains, with the exception of SUSU1, in which the wild-type copy of chromosome IX was not detected. Furthermore,

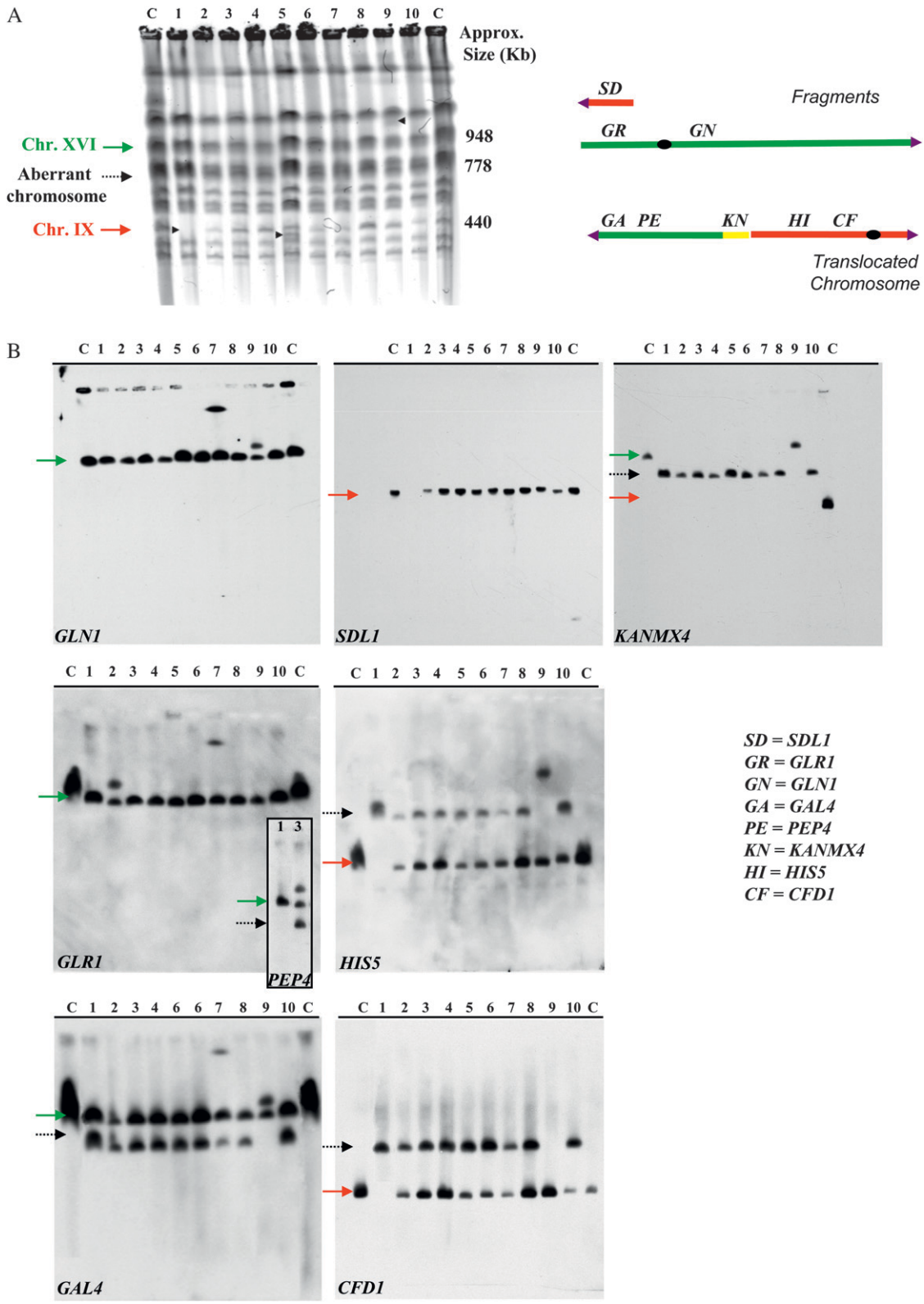

FIGURE 2.—Chromosome analysis of the SUSU translocants. (A) Chromosome separation by CHEF. Arrowheads point to visible chromosomal polymorphisms in the SUSU1, SUSU5, and SUSU9 translocants. (B) Southern blot analyses. Blots were hybridized to the labeled GAL4, PEP4, GLR1, and GLN1 probes on chromosome XVI; SDL1, HIS5, and CFD1 probes are on chromosome IX; the KANMX4 probe was use to detect the aberrant chromosome. In all Southern blots, with the exception of that hybridized with KANMX4, lane C contains San1 diploid control strain DNA. In the membrane hybridized with KANMX4, the lane C contains San1-(*DBP1/dbp1::KAN*^{R}) DNA; lane 12 contains San1-(*GUT2/gut2::KAN*^{R}) DNA. Lanes 1–10 represent DNA derived from SUSU1 to SUSU10. The adjoining PEP4-probed membrane on the GLR1 panel shows the SUSU2 chromosomal pattern in comparison to the control strain San1. All the other translocants have the same pattern as in the GAL4 panel. Red arrow: chromosome IX; dashed arrow: translocant chromosome; green arrow: chromosome XVI.

Figure 2A shows the presence of an additional polymorphism in SUSU5, which is clearly visible as an extra band between the parental chromosome III (370 kb) and chromosome IX (440 kb). This band did not hybridize with any of the probes located along chromosomes IX and XVI used in our experiments. Since a similar band was also observed in other translocants obtained in our laboratory (V. Tosato, personal communication), we cannot exclude that the event that leads to the formation of this polymorphism is not specifically correlated with the SUSU-BIT translocation events.

Gene copy-number determination: CHEF and Southern blot analysis point toward the occurrence of various mechanisms that might contribute to the rearrangement of the chromosomes participating in the translocation. To better understand the mechanisms involved in the formation of the SUSU translocants and to investigate whether aneuploidy might arise in cells that undergo BIT translocation events, we determined the copy number of certain genes located along chromosomes XVI and IX by quantitative PCR. The gene dosage of *VMR1*, located on chromosome VIII (not involved in translocation), was also determined as the control for the accuracy of our experiments. Figure 3 shows the gene dosage of the analyzed genes in the control and in the translocant strains. The results are also summarized in Figures 4 and 5.

Gene dosage experiments suggest that the consequence of the integration of the BIT cassette might also be responsible for the generation of aneuploidy in all the translocant strains. In particular, *GAL4*, *GLR1*, and *GLN1* copy-number determination showed that all the analyzed mutants have at least two copies of the wild-type chromosome XVI. In SUSU5, SUSU6, and SUSU10, the presence of three copies of this chromosome was also detected, highlighting that in the translocants a partial trisomy or tetraploidy of the fragment involved in the translocation is present. Triploid and tetraploid conditions of different parts of chromosome XVI were also detected in SUSU2, SUSU7, and SUSU9, in which Southern blot analyses revealed the presence of complex rearrangements of that chromosome. PCR data on the *SUC2* promoter, the *SUC2* ORF, and *DAL4* located on chromosome IX pointed out that in five translocants just one copy of the wild-type chromosome IX is present, whereas in SUSU3 and SUSU9 two copies are present. Three copies were detected in SUSU4 and four copies in SUSU8. In SUSU1, the absence of the wild-type copy of chromosome IX was confirmed together with the duplication of the aberrant chromosome. With the exception of this strain, the presence of only one copy of the aberrant chromosome was noted for all the other translocants by the amplification of *KANMX4*, together with *ACT1*, by using San1-*GUT2/gut2::KANMX4* as the reference strain containing one copy of the kanamycin resistance gene.

On the basis of the above observations we suggest that SUSU translocant cells carry various types of aneuploidy. Therefore, we asked whether or not such aneuploidy was a direct consequence of targeted translocation and associated rearrangement of chromosomal fragments. To this end, we analyzed the presence of such aneuploidy in strains that carried ectopic integration of the SUSU-BIT construct and were previously obtained with both LiAc and spheroplast transformation methods. qPCR data for gene copy-number determination of *SUC2* and *DAL4* located on chromosome IX, and for *GLR1* and *GAL4* located on chromosome XVI, demonstrated that both chromosomes are present in two copies (wild-type configuration) in all the four ectopic integrants (see Figure S2). These observations suggest that the transformation process itself, or the BIT integration *per se*, cannot account for the rearrangements observed in the SUSU translocant strains (Figure S2).

Physiological and morphological characteristics of the SUSU translocants: Because we noted genotypic variations among the translocants, we asked whether or not they are also expressed as physiological and morphological differences.

Growth test on carbon sources: First, we analyzed the fitness and the ability of the SUSU translocants to grow in different carbon sources both on plates (not shown) and in liquid medium. Results plotted in Figure S1 show that, in all the carbon sources tested, the SUSU translocants reached the stationary phase at lower culture density than the parental strain San1. This phenomenon was notably evident when the mutant strains were cultured on the nonfermentable carbon source glycerol. In particular, SUSU5 was completely unable to grow on glycerol and also in other respirable-only carbon sources, such as ethanol and acetate, indicating the presence of some defect in the respiration and/or mitochondrial metabolism. The low fitness of SUSU9 on glucose and of SUSU1 on raffinose was also noteworthy. From the physiological point of view, we also noted that some strains, such as SUSU2, −6, −7, −8, and −9, were characterized by their strong ability to flocculate whereas some others were not (not shown).

Results summarized in Table 1 indicate that only 7 of 10 mutants exhibit sufficient sporulation, SUSU9 being the translocant with the highest sporulation efficiency (79% of the control strain San1) and SUSU4 the mutant strain with the lowest efficiency (2% of the control strain).

Morphology: The morphology of the cells was monitored during cultivation on YPD medium and analyzed after 16, 40, and 64 hr by light fluorescence microscopy following DAPI staining. These assays highlighted that the SUSU translocant cell populations exhibit the highest percentage (2–5% of the total cell population) of morphological defects after 40 hr of growth on rich medium. After this time, the number of abnormal cells,

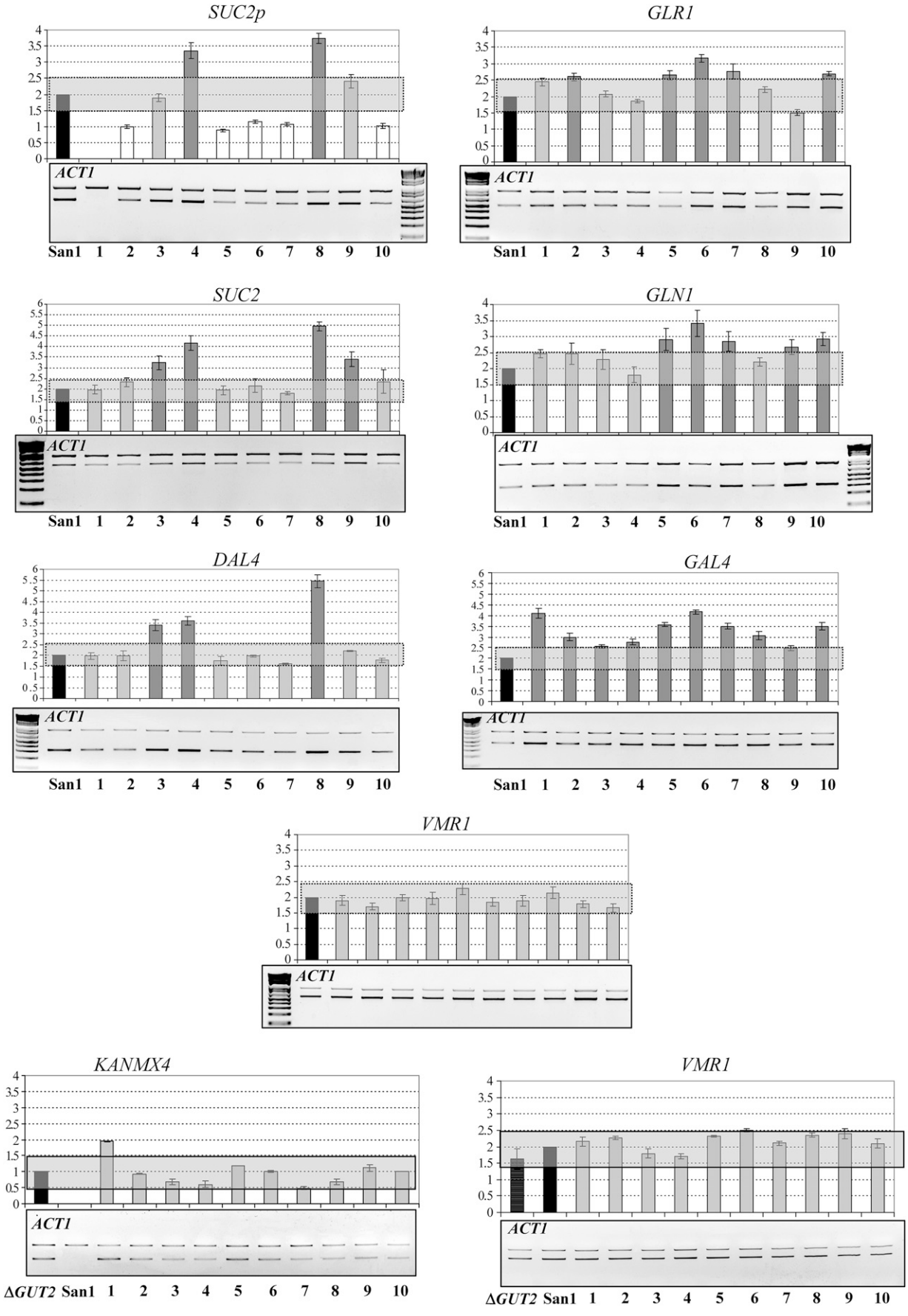
SUC2p
ACT1
San1 1 2 3 4 5 6 7 8 9 10
GLR1
ACT1
San1 1 2 3 4 5 6 7 8 9 10
SUC2
ACT1
San1 1 2 3 4 5 6 7 8 9 10
GLN1
ACT1
San1 1 2 3 4 5 6 7 8 9 10
DAL4
ACT1
San1 1 2 3 4 5 6 7 8 9 10
GAL4
ACT1
San1 1 2 3 4 5 6 7 8 9 10
VMR1
ACT1
KANMX4
ACT1
ΔGUT2 San1 1 2 3 4 5 6 7 8 9 10
VMR1
ACT1
ΔGUT2 San1 1 2 3 4 5 6 7 8 9 10

as well as the number of actively dividing cells, decreases in all strains (data not shown). Figure 6 shows a few examples of the abnormal cell morphologies observed under the microscope, such as germination tube formation, pseudohyphal growth, multi-budded cells, and cells with elongated buds, all indicative of cell cycle defects. It is worth noting that the percentage of all these defects is much lower than that found in other translocants previously described, in which they were between 10 and 20% of the cell population (Nikitin *et al.* 2008). As in previous translocants obtained with the BIT system (Nikitin *et al.* 2008), defects in karyokinesis are also evident in most of the SUSU strains (Figure 6).

Viability and cell cycle regulation: The FUN-1 stain solution is a fluorescent vital dye useful for distinguishing between metabolically active/alive yeast cells (forming CIVSs; Figure 7B) and dead/not metabolically active cells (yellow cells in Figure 7B). We used this staining method to analyze the viability of the SUSU translocants at the late exponential phase. All comparisons were made using the parental San1 strain as reference (Figure 7, A and B).

As expected, a very low percentage (1%) of cell mortality in San1 cells was reached after 18 hr of growth on YPD, whereas higher mortality was noted in all the SUSU translocants (Figure 7A). In half of the translocants analyzed, the percentage of non-metabolic active/dead cells is >10% (*i.e.*, ~10 times more than the control strain). The highest percentage of such cells was found in SUSU9 (21%). In agreement with these data, we observed that SUSU9 had very low fitness in YPD medium correlated to a maximum optical density of 1.36 OD_{600} corresponding to 1.8×10^7 cells/ml, observed for this strain. On the other hand, SUSU5 was the strain with the lowest percentage of mortality in the late exponential phase (2%). Another interesting feature characteristic of certain SUSU mutants observed by FUN-1 vital staining was the presence of some mother cells attached to a dead bud. This could be explained by the presence of defects in nuclear segregation described earlier (see Figure 6).

Expression analysis: On the basis of the above morphological and physiological differences among the SUSU translocants, we focused on elucidating these differences at the level of gene expression. Using semiquantitative RT–PCR, we analyzed the expression of the genes located along the two chromosomes involved in the translocation. In addition, we also analyzed the expression profile of a set of genes involved in various cellular processes such as cell cycle regulation, oxidative stress response, apoptosis, and multidrug resistance. The names of the analyzed genes are reported in Figure 8 and in Table S3. As in previous expression analyses of BIT translocants, *HSC82* was chosen as a constitutive control gene (Nikitin *et al.* 2008; Tosato *et al.* 2009). For all the genes analyzed, an expression level higher than twice, or equal to or lower than half, the expression level of the control strain San1, was considered as a significant up- or downregulation of transcription, respectively. Figure 8 describes the expression patterns of all the analyzed genes in the 10 SUSU translocants grown on YPD medium. The histograms show that *CLB1* and the arginase *CAR1* are the only two genes with an expression level similar to that of the control strain in all 10 SUSU translocants whereas all the other genes are up- or downregulated in some of the mutant strains. Indeed, *SSU1* expression data clearly demonstrate that, despite the triploid or tetraploid condition of this gene in the SUSU translocants (Figures 4 and 5), its expression was similar to the control strain in most of the SUSU strains with the exception of SUSU3, SUSU6, and SUSU10. In these strains, expression level was ~3-fold less, and 7.5- and 2.5-fold more than in the control, respectively. The greater increase of *SSU1* expression in SUSU6 and SUSU10 cannot be correlated only to the detection of four copies of the chromosomal arm harboring this gene in these two strains (Figures 4 and 5), since a similar tetraploid condition in SUSU1 and SUSU5 exhibited a wild-type expression level. Thus, other factors such as physiological conditions or the presence of unbalanced cellular components due to the effect of translocation and/or the ensuing aneuploidy condition might be responsible for its strong activation in SUSU6 and SUSU10 strains.

The expression of *SUC2* was analyzed on both glucose (repressing condition; Figure 8) and raffinose (dere-

Figure 3.—Quantitative PCR copy-number analysis of genes located on chromosomes XVI and IX. In each gel, the higher band corresponds to that of the *ACT1* control gene amplicon in chromosome VI, whereas the lower band corresponds to the amplicon of the analyzed gene involved in the translocation. The gene dosage of *VMR1*, located on chromosome VIII, but not involved in translocation, was also determined as the control for the accuracy of our experiments. Each analyzed gene and *ACT1* were co-amplified in the same PCR reaction. *KANMX4* quantification was performed with genomic DNA from San1-*GUT2/gut2::KANMX4* containing one copy of the *KANMX4* gene. ΔGUT2, San1-*GUT2/gut2::KANMX4* - control strain; San1, original parental strain; 1–10: the 10 SUSU translocants. Values presented on the graph above the gels show the gene dosage expressed as an average of at least three independent densitometric determinations from four gels. Data normalized with respect to *ACT1* considered as a two-copy-number gene were then compared with the normalized values in the diploid San1 control strain. San1, control strain; 1–10: the 10 SUSU translocants. Gray rectangles highlight a ±0.5 variation in gene copy number. Variations within this interval were considered as insignificant variation in gene copy number with respect to the wild-type situation. Solid bars: San1 control strain; open bars: gene copy number lower than the control strain; lightly shaded bars: gene copy number equal to that of the control strain; darkly shaded bars: gene copy number higher than that of the control strain.

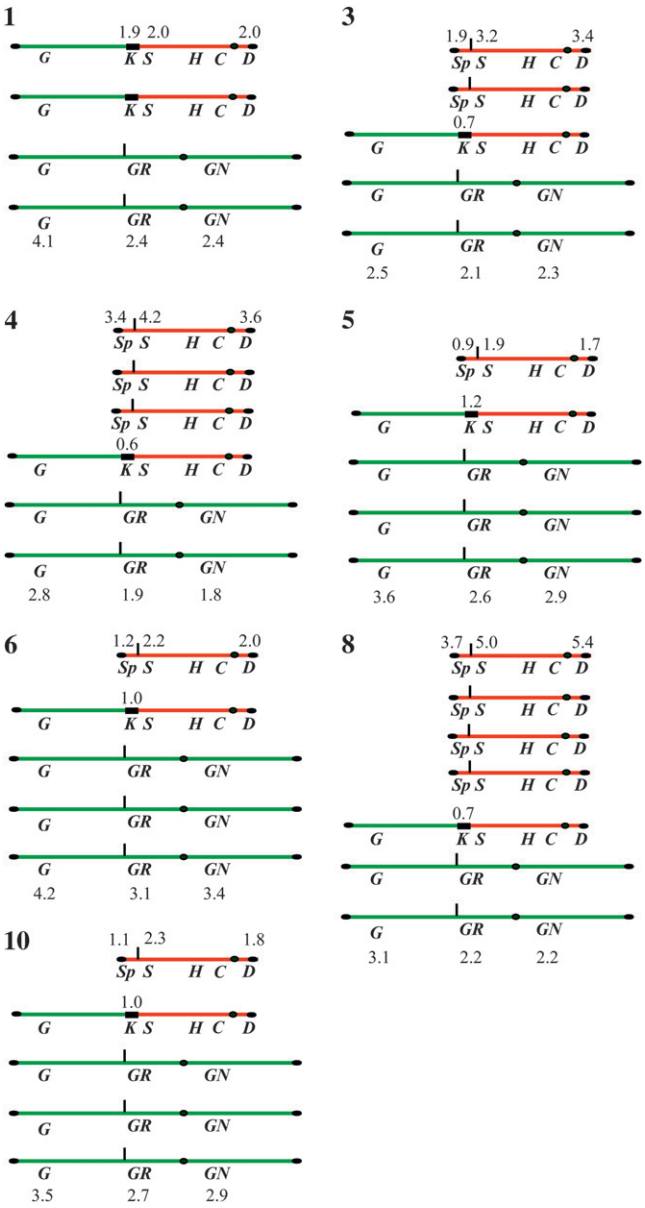

FIGURE 4.—Summary of the genotypic situation of chromosomes XVI and IX in the seven SUSU translocants carrying no complex rearrangements. The genes analyzed in the Southern blot and in the gene copy-number experiments are reported. Gene copy-number values are also indicated. G, *GAL4*; GR, *GLR1*; GN, *GLN1*; S, *SUC2*; Sp, *SUC2* promoter; H, *HIS5*; C, *CFN1*; D, *DAL4*; K, *KANMX4*. Numbers 1, 3, 4, 5, 6, 8, and 10 indicate SUSU1, SUSU3, SUSU4, SUSU5, SUSU6, SUSU8, and SUSU10 strains, respectively.

pressing condition; see also Figure S3) (LUTFIYYA and JOHNSTON 1996; OZCAN *et al.* 1997) to study the effect of the translocation not only on the basal expression level of this gene but also on its transcriptional activation. In fact, the translocation breakpoints lie within a key position of the *SUC2* promoter region, *i.e.*, a few nucleotides upstream from its activation DNA-binding sites and inside a nucleosome that is lost during gene transcription activation (FLEMING and PENNINGS 2007).

Figure 8 and Figure S3 show that the basal expression level of *SUC2* is similar to that of the control strain in all the translocants with the exception of SUSU5, in which the expression of this gene is ~5-fold less. On the other hand, the induction of *SUC2* is impaired in many, but not all, translocants, in which under activating conditions the expression level of the gene is 10-fold less in SUSU1, SUSU6, and SUSU8, reduced 3-fold in SUSU7, SUSU9, and SUSU10, or halved in SUSU3. Differences in *SUC2* activation levels can be explained on the basis of different genotypes and other secondary factors such as different intracellular physiological conditions. Interestingly, we found a strong reduction of the *SUC2* mRNA level despite *SUC2* diploid and polyploid status in various translocants. Thus, as for *SSU1*, gene copy number by itself cannot account for variations in gene expression patterns in the above-mentioned translocants.

Results summarized in Figure 8 also demonstrate that the increased gene expression at the translocation breakpoint and along the translocated chromosome observed in the BIT translocants previously described (NIKITIN *et al.* 2008) was not a common feature of all the SUSU mutant strains. In fact, SUSU2 and SUSU3 did not show any significant alteration in the transcription level of the genes analyzed. The only alteration observed in these translocants was the previously described underexpression of *SSU1* and of *RRD1* located on chromosome IX.

Three strains, SUSU1, SUSU4, and especially SUSU6, showed strong variability in the expression of many genes, suggesting a larger alteration of their physiology and metabolism. In SUSU1, we observed a 2.1-fold increase in the mRNA level of *GAL4* located on chromosome XVI and a 3.5-fold increase of the multidrug-resistant gene *VMR1* transcript. In the same strain, we also found the overexpression of the caspase *YCA1* gene and of *GSH1*, which is also involved in apoptosis and cellular response to oxidative stress. Interestingly, previous authors (TOSATO *et al.* 2009; D. NIKITIN personal communication) have revealed that *VMR1* upregulation was also present in other homologous and heterologous BIT translocants.

The three genes mentioned above (*GSH1*, *YCA1*, and *VMR1*) are also highly overexpressed in SUSU6, which is characterized by a strong deregulation of the transcription of almost all the analyzed genes with the exceptions of *CAR1*, *SUC2*, *MUC1*, and *CLB1*. In particular, in addition to the three genes mentioned above, the two genes located on both sides of the translocation breakpoint on chromosome XVI showed a pronounced increase in their steady mRNA levels (7.6- and 3.8-fold mRNA levels increasing for *SSU1* and *GLR1*, respectively). The overexpression of *GLR1*, encoding the cytosolic and mitochondrial glutathione oxidoreductase, can be correlated to the increased *GSH1* transcription and could indicate oxidative stress conditions generated within SUSU6 cells. At the same time, over-

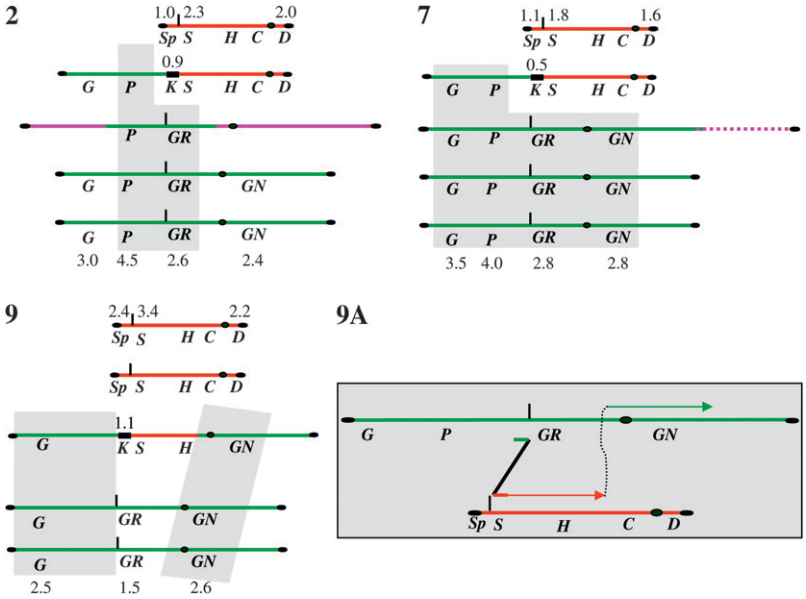

FIGURE 5.—Summary of the genotype of chromosomes XVI and IX in three SUSU translocants harboring complex rearrangements. As in Figure 4, numbers 2, 7, and 9 indicate SUSU2, SUSU7, and SUSU9 strains, respectively. The scheme contained in panel 9A shows a putative template switching-like mechanism that might be responsible for the rearrangement observed in SUSU9 (see RESULTS and DISCUSSION for more details).

expression of *YCA1* suggests that an apoptotic response might be activated in this strain. The overexpression of the cell cycle-related gene *CDC48* in this strain is an indication of the presence of cell cycle defects. Among other genes analyzed, only *RRD1* was downregulated in SUSU6. In the SUSU5 strain, which exhibits a petite phenotype, two of the analyzed genes—*SUC2* (see above) and *GSH1*—showed a reduced level of mRNA in comparison to the control strain, which for the latter was ~4-fold less than that of the control.

In summary, our results show a heterogeneous situation in many SUSU translocants in which some genes are activated, others are downregulated, and others have the same expression level of the control strain. This may or may not correlate with the copy number of these genes, suggesting a more intricate adaptation of the cells to a dramatically changed karyotype.

DISCUSSION

Translocation events not only are gross chromosomal rearrangements that can be associated with cancer development in mammalian cells and acquisition of deleterious phenotypes in eukaryotic microorganisms, but also are a powerful evolutionary force capable of strongly reshaping the genome. For example, translocation events have been associated with the acquisition of advantageous antifungal drug resistance in the yeast *Candida glabrata* (POLAKOVA *et al.* 2009). Despite their importance for the maintenance and evolution of genome organization, little is known about the molecular mechanisms and pathways involved in the formation and regulation of a translocation event.

In this work, we have used the BIT system (TOSATO *et al.* 2005) to generate a collection of mutant yeast strains harboring the same translocation between chromosomes XVI and IX (Figure 1). Southern blot analysis and gene copy-number determination revealed that the integration of the SUSU linear DNA cassette can induce the formation of not only a non-reciprocal translocation, but also triggers other complex rearrangements generating different types of aneuploidy in all the mutant strains analyzed. This complex abnormal karyotype bearing monosomy, disomy, and trisomy for different segments of the translocation participants is strongly reminiscent of what is described (PEDERSEN *et al.* 2000) in leukemia patients carrying unbalanced translocations. Even though *S. cerevisiae* tolerates aneuploidy well, it is common knowledge that aneuploidy has severe effects on growth and development, as also reported in baker's yeast (TORRES *et al.* 2007). Mainte-

TABLE 1

Sporulation efficiency

Strain	% sporulation efficiency
San1	100
SUSU1	ND
SUSU2	20
SUSU3	35
SUSU4	2
SUSU5	ND
SUSU6	20
SUSU7	ND
SUSU8	22
SUSU9	79
SUSU10	49

The sporulation efficency of the mutant strains is expressed in comparison to the sporulation efficency of the control strain considered as 100%. SUSU1 and SUSU7 strains are not able to sporulate. ND, not detected.

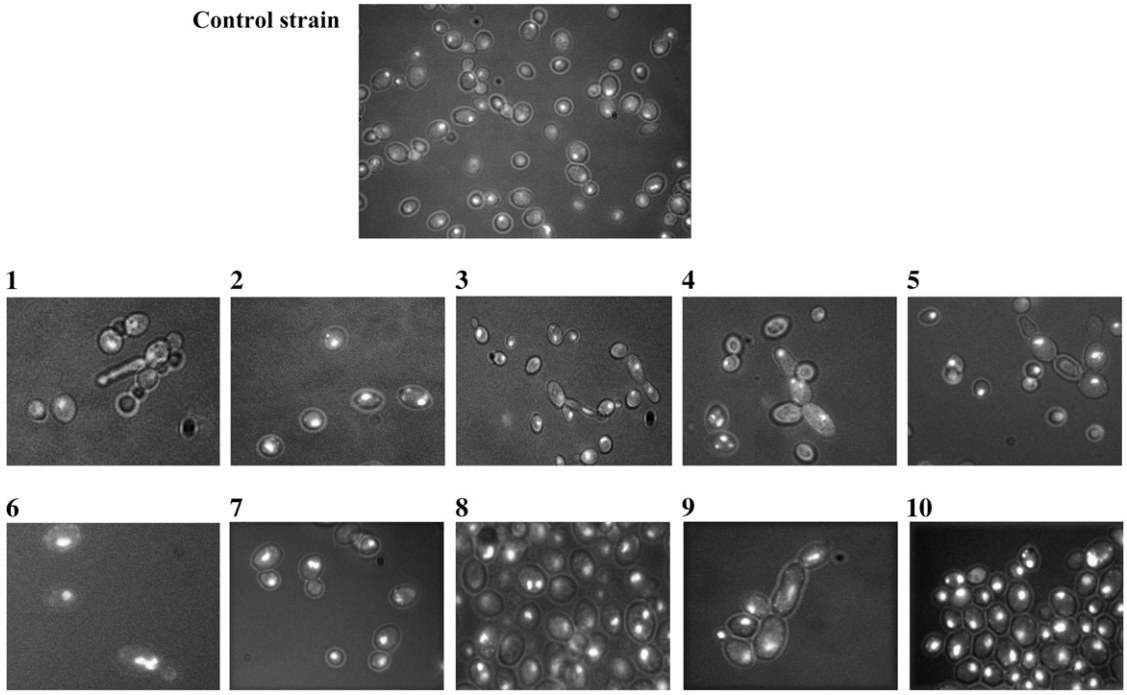

Figure 6.—Microphotography of DAPI-stained control strain cells and SUSU translocants. (1–10) SUSU1–SUSU10 translocant cells. Various abnormal cell morphologies and karyokinetic defects are shown: germination tube formation (1), pseudohyphal growth of cells (4, 5, and 9), and multi-budded cells or cells with elongated buds (3 and 4). Nuclear fragmentation and/or defects in nuclear segregation are evident in some of the cells shown in each field (2, 4, 5, 6, 7, 8, and 10).

nance of euploidy is essential for survival of a species, and correlations between cancer and aneuploidy were reported in 1890 by D. P. von Hansemann and in 1902 by T. Boveri (Bignold *et al.* 2006). Recently, aneuploidy was proposed to be the major pre-neoplastic condition leading to chromosome instability and promoting transformation of the normal cells (Duesberg *et al.* 2005). Variations in chromosome numbers and aneuploidy formation are thus usually strongly inhibited by checkpoint mechanisms. In the SUSU mutant strains, such cellular surveillance seems to be bypassed, leading to the formation of gross chromosomal rearrangements possibly by various mechanisms.

One possible mechanism for recombination-associated generation of aneuploidy is BIR (Morrow *et al.* 1997; Jain *et al.* 2009). This process can well explain the partial trisomy of chromosome XVI present in SUSU3, SUSU4, and SUSU8. According to the two-step integration model of the BIT cassette proposed for other translocants previously described (Tosato *et al.* 2005), we might hypothesize that in these mutants the cassette initially integrates at the *SUC2* locus via homologous recombination and then, in a second step, completes the integration at the *SSU1* locus by strand invasion and synthesis toward the telomere. This model is also supported by the fact that the integration of the BIT cassette might mimic the condition in which homology is limited to one end of the DSB, a condition that strongly favors the repair of a break by the BIR mechanism (Malkova *et al.* 2005; Vanhulle *et al.* 2007; Jain *et al.* 2009). However, we cannot explain the partial trisomy of chromosome IX observed in the SUSU3 strain by a BIR-like event, as it is known that the BIR replication apparatus is blocked at the centromere (Morrow *et al.* 1997). One possible explanation of this situation is that during the integration of the BIT cassette an alternative replication apparatus capable of passing through the centromeric region might be involved, giving rise to a complete and functional chromosome. A striking observation of an ~10-fold increase in the occurrence of a translocation event, upon transforming S-phase blocked yeast cells with the BIT construct, has recently been noted in our laboratory (V. Tosato, personal communication). Indeed, recent research reveals that a non-reciprocal translocation, leading to duplication of chromosomal regions, can also arise from an unconventional Pol32-independent, BIR-like mechanism (Putnam *et al.* 2009) This suggests that formation of complex rearrangements might occur by different mechanisms capable of repair by DNA synthesis. Furthermore, in support of this view, recent observations in our group show that deletion of *POL32* does not affect the rate of BIT translocation induction (V. Tosato, unpublished data). This hypothesis, however, does not provide an exhaustive explanation of all the rearrangements depicted in Figures 4 and 5. In particular, an explanation of the multiplication of chromosome IX in SUSU4 and SUSU8 strains or of

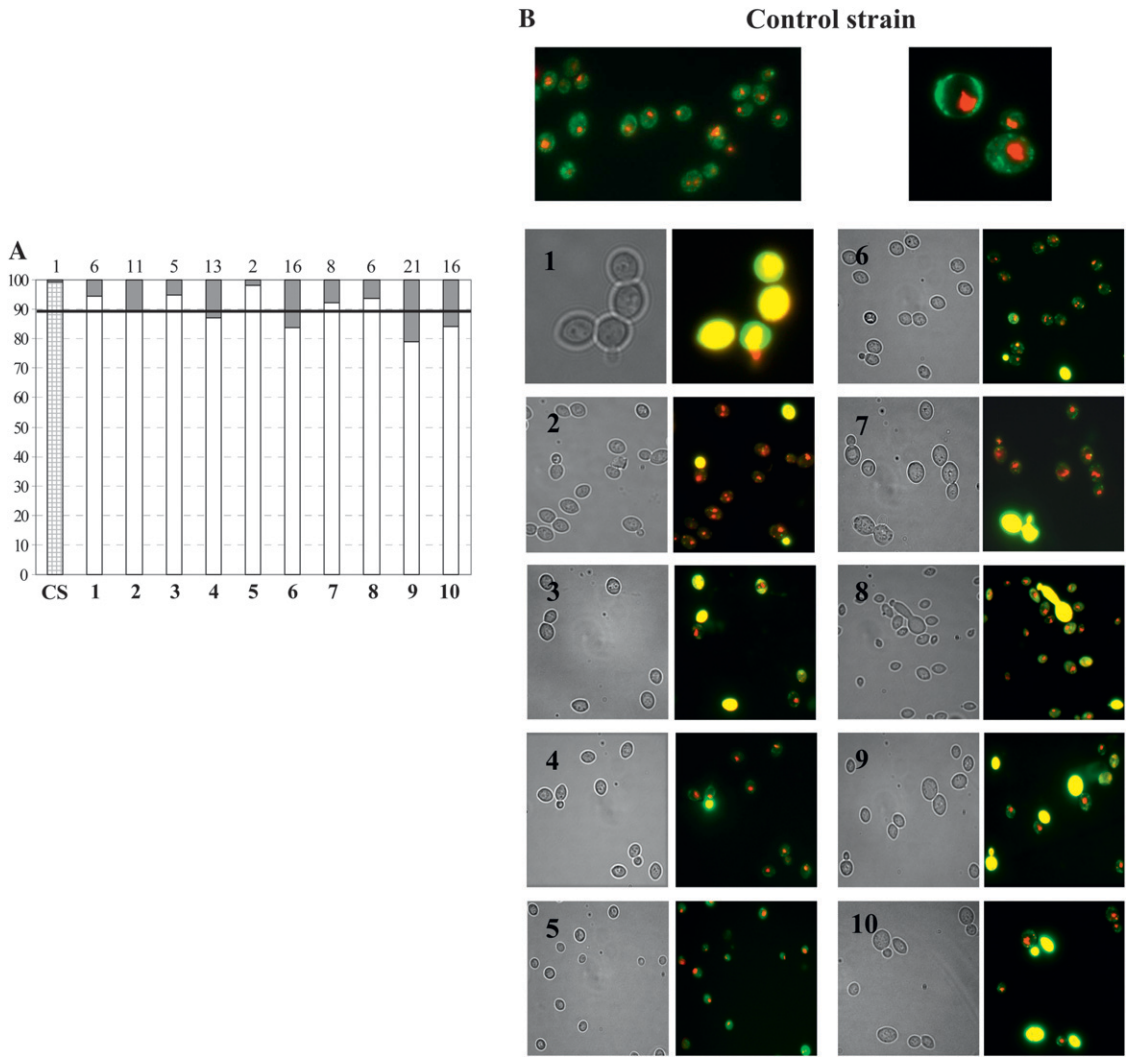

Figure 7.—Viability test. (A) Representation of the percentage of dead cells at the late exponential phase of growth. The exact percentage of dead cells of each strain is reported on the top of the graph and is represented by shading on the bars. The dark horizontal line indicates the 10% value. CS: control strain; bars 1–10: SUSU1–SUSU10 translocants. (B) Fluorescence microphotography of FUN1-stained cells. Metabolically active/alive yeast cells containing CIVSs and dead/not metabolically active cells are shown in yellow. (1–10) SUSU1–SUSU10 translocants.

the triplication of chromosome XVI in SUSU5, SUSU6, and SUSU10 strains cannot be based on such a hypothesis. Another explanation for these phenomena could be that, in adapted cells that are able to bypass cell cycle arrest, the recombination of the BIT cassette interferes with chromosome segregation during mitosis, giving rise to the aneuploidy noted for both chromosomes XVI and IX. Missegregation due to interchromosomal association as described (Kaye *et al.* 2004) was also proposed to be linked to the generation of disomic cells following the integration of a DNA construct with short heterologous termini in *S. cerevisiae* (Svetec *et al.* 2007). A defect in chromosome segregation, possibly due to the size differences of chromosome IX and the newly formed aberrant chromosome, might account for the duplication or triplication of chromosome IX observed in the SUSU4 and SUSU8 strains. Indeed, perhaps unable to identify the remaining portion of chromosome IX, the cells could behave as monosomic for that chromosome, restoring a euploid situation by endo-reduplication with a mechanism similar to that already described (Waghmare and Bruschi 2005). Defects in chromosome IX segregation that lead to the loss of the wild-type copy of chromosome IX followed by the duplication of the translocant chromosome can also explain the karyotype of SUSU1, although a double translocation event leading to such a karyotype cannot be ruled out. It is noteworthy that in SUSU1 there is a loss of genetic material. In fact, it lacks all the genes contained in the 36,685-bp fragment located on the subtelomeric region upstream from the *SUC2* locus. All these genes are nonessential.

Complex rearrangements involving chromosome XVI have been described in SUSU2, SUSU7, and SUSU9

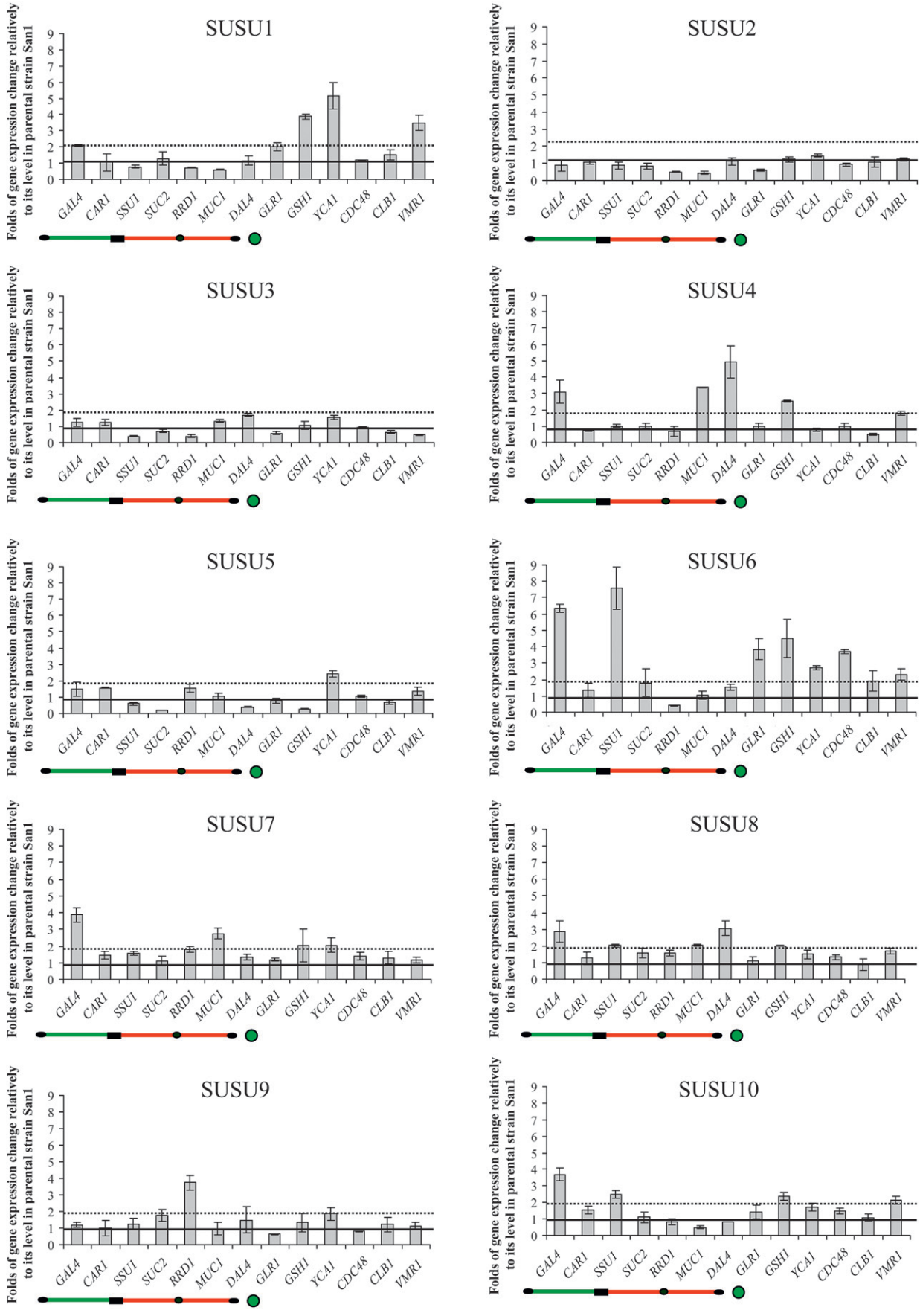
SUSU1
SUSU2
SUSU3
SUSU4
SUSU5
SUSU6
SUSU7
SUSU8
SUSU9
SUSU10
Folds of gene expression change relatively to its level in parental strain San1
0 1 2 3 4 5 6 7 8 9
GAL4 CAR1 SSU1 SUC2 RRD1 MUC1 DAL4 GLR1 GSH1 YCA1 CDC48 CLB1 VMR1

(Figure 5). In particular, the SUSU9 strain does not possess the expected translocant chromosome but instead a different aberrant chromosome in which only a small part of chromosome IX was rearranged together with chromosome XVI. The configuration of this chromosome strongly suggests that a template switching-like mechanism, similar to the FoSTeS described in mammalian cells (Lee *et al.* 2007), might be responsible for this rearrangement. We hypothesize that in this mutant the cassette first integrates at the *SSU1* locus via homologous recombination and then completes the integration at the *SUC2* locus by strand invasion and synthesis (or break-induced replication). After this starting event, we suppose a stalling of the replication fork before the centromere of chromosome IX is followed by template dissociation and re-invasion of chromosome XVI and new DNA synthesis to the end of chromosome XVI, leading to the chromosome configuration described earlier (Figure 5, panel 9A).

Overall, our data also demonstrate that the integration of the linear DNA fragment into the yeast genome can be a great force for evolution. In fact, in our experiments, the integration of the same cassette at the two target loci was processed in eight different ways, generating strains different in karyotype and consequently in phenotype and physiology. This variety of morphologies and phenotypes and the variation of the expression level of various genes among the different translocants were not observed in strains carrying Kan^r integration on individual chromosomes at the translocation breakpoint (see Figure S4). This observation suggests that the mere integration of *KANMX4* by itself does not destabilize and deregulate gene expression or other physiological aspects such as sporulation, flocculation (not shown), or growth rate.

Some of the mutant phenotypes described in this work, such as the presence of a slow growth rate, morphological aberrations, and defects in nuclear segregation, are similar to those recently illustrated for the D10*big* and *small* mutants carrying a translocation between chromosomes VIII and XV (Nikitin *et al.* 2008). However, the overexpression of the genes located at the translocation breakpoints typical of the D10 mutant is not observed in most of the SUSU translocants. This suggests that the effect of a translocation on gene expression might be locus-specific, *i.e.*, dependent on the loci and on the chromosomes involved in BIT. Moreover, in the SUSU translocants the presence of aneuploidy, previously not detected in D10*big* and *small* mutants, might also influence global gene expression. Torres *et al.* (2007) recently demonstrated that aneuploidy causes a transcriptional response with the doubling of gene expression along the entire length of a disomic chromosome. In SUSU strains, increased mRNA levels of genes present in a higher copy number, in comparison to the control strain, were observed in some of the mutants (Figure 8) but not in others. Perhaps in these mutants a combination of two effects, translocation and aneuploidy, is established at later time point after translocation. On the other hand, many phenotypic characteristics of the aneuploid strains described by Torres and colleagues were also found in these mutant strains, such as slow growth rate (probably also in this case because of a nonspecific disruption of the cellular homeostasis), lower OD_{600} values of mutants noted in the stationary phase with respect to the control strain, proliferation defects, and an increased number of G_1 phase-stopped cells (data not shown).

Interestingly, some of the SUSU translocants showed the overexpression of *YCA1*, suggesting the activation of apoptotic pathways. The genes *GSH1* and *GLR1* involved in oxidative stress response were also overexpressed in some of the translocant strains together with the multidrug resistance gene *VMR1*, which is homologous to the ABCC-type multi-drug transport proteins. This gene was also overexpressed in other BIT translocants between both heterologous and homologous chromosomes (Tosato *et al.* 2009; D. Nikitin, personal communication). The common overexpression of this gene in our translocants and the documented overexpression of the homologous human Mrp4p in some aggressive primary neuroblastomas, also characterized by unbalanced chromosomal translocations (Janoueix-Lerosey *et al.* 2005; Norris *et al.* 2005), suggest that the overexpression of this gene might be considered as a general effect of these kinds of aberrations. In this view, the detection of generally shared mutant phenotypes among translocants will have to be analyzed to clarify their dependence or independence from the specific breakpoints. It could be also interesting to know if the ectopic insertion of one of the homologies on a different chromosome could be used efficiently for a homologous repair, which would generate a reciprocal translocation. We think that the BIT system provides a valuable tool for obtaining statistically significant numbers of different translocation mutants without prior genomic engineering of cells. Results presented in this work also suggest that BIT could be considered as an

Figure 8.—Semiquantitative RT–PCR analysis of the SUSU translocants. Graphs of the expression level of various genes located along the translocated chromosome or those involved in various cellular processes of *S. cerevisiae*. The names of the analyzed genes are reported below each bar (see also Table S3). Values reported in the graphs represent the expression level of each gene normalized with the expression level of the control gene *HSC82* and then compared with the normalized expression of the analyzed gene in the San1 control strain considered as the unit (horizontal black line). Dotted black line represents a twofold increase in gene expression relative to the expression level in the parental strain. The scheme of the translocated chromosome shown below each graph indicates the relative position of the genes along this chromosome. The green circle below *GLR1* indicates its presence on chromosome XVI but not on the translocated chromosome.

experimentally reliable system to mimic the spontaneous mitotic translocation of higher eukaryotic cells. In fact, as observed by others in mammalian cells, our findings strongly support that aneuploidy arising from an initial nonreciprocal translocation event may generate a heterogeneous population of mutant cells that are phenotypically and genotypically diverse. At the same time, our laboratory recently showed that near-reciprocal translocation between homologous chromosomes does not affect gene expression at the genomic loci flanking the breakpoints (Tosato *et al.* 2009).

We thank Valentina Tosato and Dmitri Nikitin for help and useful discussions throughout the experimental work as well as for help with the preparation of the manuscript. We also thank Michela Ronzani for technical help. Beatrice Rossi is an International Centre for Genetic Engineering and Biotechnology (ICGEB) Post-doctoral Fellow, and Pawan Noel is a Ph.D. Fellow supported by the ICGEB doctoral program.

LITERATURE CITED

Agarwal, S., A. A. Tafel and R. Kanaar, 2006 DNA double-strand break repair and chromosome translocations. DNA Repair (Amst.) **5:** 1075–1081.

Avram, D., and A. T. Bakalinsky, 1997 *SSU1* encodes a plasma membrane protein with a central role in a network of proteins conferring sulfite tolerance in *Saccharomyces cerevisiae*. J. Bacteriol. **179:** 5971–5974.

Aylon, Y., and M. Kupiec, 2004 New insights into the mechanism of homologous recombination in yeast. Mutat. Res. **566:** 231–248.

Bernstein, R., 1988 Cytogenetics of chronic myelogenous leukemia. Semin. Hematol. **25:** 20–34.

Bignold, L. P., B. L. Coghlan and H. P. Jersmann, 2006 Hansemann, Boveri, chromosomes and the gametogenesis-related theories of tumours. Cell Biol. Int. **30:** 640–644.

Bosco, G., and J. E. Haber, 1998 Chromosome break-induced DNA replication leads to nonreciprocal translocations and telomere capture. Genetics **150:** 1037–1047.

Dalla-Favera, R., M. Bregni, J. Erikson, D. Patterson, R. C. Gallo *et al.*, 1982 Human c-myc onc gene is located on the region of chromosome 8 that is translocated in Burkitt lymphoma cells. Proc. Natl. Acad. Sci. USA **79:** 7824–7827.

De Braekeleer E., N. Douet-Guilbert, M. J. Le Bris, F. Morel, M. De Braekeleer, 2007 Translocation 3;21 trisomy 8, and duplication of the Philadelphia chromosome: a rare recurrent cytogenetic pathway in the blastic phase of chronic myeloid leukemia. Cancer Genet. Cytogenet. **179:** 159–161.

Delneri, D., I. Colson, S. Grammenoudi, I. N. Roberts, E. J. Louis *et al.*, 2003 Engineering evolution to study speciation in yeasts. Nature **422:** 68–72.

Duesberg, P., R. Li, A. Fabarius and R. Hehlmann, 2005 The chromosomal basis of cancer. Cell. Oncol. **27:** 293–318.

Egli, D., E. Hafen and W. Schaffner, 2004 An efficient method to generate chromosomal rearrangements by targeted DNA double-strand breaks in *Drosophila melanogaster*. Genome Res. **14:** 1382–1393.

Fleming, A. B., and S. Pennings, 2007 Tup1-Ssn6 and Swi-Snf remodelling activities influence long-range chromatin organization upstream of the yeast *SUC2* gene. Nucleic Acids Res. **35:** 5520–5531.

Gasparini, P., G. Sozzi and M. A. Pierotti, 2007 The role of chromosomal alterations in human cancer development. J. Cell Biochem. **102:** 320–331.

Gu, W., F. Zhang and J. R. Lupski, 2008 Mechanisms for human genomic rearrangements. Pathogenetics **1:** 4.

Haber, J. E., 2006 Transpositions and translocations induced by site-specific double-strand breaks in budding yeast. DNA Repair (Amst.) **5:** 998–1009.

Heale, S. M., L. I. Stateva and S. G. Oliver, 1994 Introduction of YACs into intact yeast cells by a procedure which shows low levels of recombinagenicity and co-transformation. Nucleic Acids Res. **22:** 5011–5015.

Jain, S., N. Sugawara, J. Lydeard, M. Vaze, N. Tanguy Le Gac *et al.*, 2009 A recombination execution checkpoint regulates the choice of homologous recombination pathway during DNA double-strand break repair. Genes Dev. **23:** 291–303.

Janoueix-Lerosey, I., P. Hupe, Z. Maciorowski, P. La Rosa, G. Schleiermacher *et al.*, 2005 Preferential occurrence of chromosome breakpoints within early replicating regions in neuroblastoma. Cell Cycle **4:** 1842–1846.

Kaiser, C., S. Michaelis and A. Mitchell, 1994 *Methods in Yeast Genetics*. Cold Spring Harbor Laboratory Press, Cold Spring Harbor, NY.

Kanaar, R., J. H. Hoeijmakers and D. C. van Gent, 1998 Molecular mechanisms of DNA double strand break repair. Trends Cell Biol. **8:** 483–489.

Kaye, J. A., J. A. Melo, S. K. Cheung, M. B. Vaze, J. E. Haber *et al.*, 2004 DNA breaks promote genomic instability by impeding proper chromosome segregation. Curr. Biol. **14:** 2096–2106.

Lee, J. A., C. M. Carvalho and J. R. Lupski, 2007 A DNA replication mechanism for generating nonrecurrent rearrangements associated with genomic disorders. Cell **131:** 1235–1247.

Lutfiyya, L. L., and M. Johnston, 1996 Two zinc-finger-containing repressors are responsible for glucose repression of *SUC2* expression. Mol. Cell. Biol. **16:** 4790–4797.

Malkova, A., M. L. Naylor, M. Yamaguchi, G. Ira and J. E. Haber, 2005 *RAD51*-dependent break-induced replication differs in kinetics and checkpoint responses from *RAD51*-mediated gene conversion. Mol. Cell. Biol. **25:** 933–944.

Millard, P. J., B. L. Roth, H. P. Thi, S. T. Yue and R. P. Haugland, 1997 Development of the FUN-1 family of fluorescent probes for vacuole labeling and viability testing of yeasts. Appl. Environ. Microbiol. **63:** 2897–2905.

Morrow, D. M., C. Connelly and P. Hieter, 1997 "Break copy" duplication: a model for chromosome fragment formation in *Saccharomyces cerevisiae*. Genetics **147:** 371–382.

Motegi, A., and K. Myung, 2007 Measuring the rate of gross chromosomal rearrangements in *Saccharomyces cerevisiae*: a practical approach to study genomic rearrangements observed in cancer. Methods **41:** 168–176.

Motegi, A., K. Kuntz, A. Majeed, S. Smith and K. Myung, 2006 Regulation of gross chromosomal rearrangements by ubiquitin and SUMO ligases in *Saccharomyces cerevisiae*. Mol. Cell. Biol. **26:** 1424–1433.

Muehleck, S. D., R. W. McKenna, D. C. Arthur, J. L. Parkin and R. D. Brunning, 1984 Transformation of chronic myelogenous leukemia: clinical, morphologic, and cytogenetic features. Am. J. Clin. Pathol. **82:** 1–14.

Nickoloff, J. A., L. P. De Haro, J. Wray and R. Hromas, 2008 Mechanisms of leukemia translocations. Curr. Opin. Hematol. **15:** 338–345.

Nikitin, D., V. Tosato, A. B. Zavec and C. V. Bruschi, 2008 Cellular and molecular effects of nonreciprocal chromosome translocations in *Saccharomyces cerevisiae*. Proc. Natl. Acad. Sci. USA **105:** 9703–9708.

Norris, M. D., J. Smith, K. Tanabe, P. Tobin, C. Flemming *et al.*, 2005 Expression of multidrug transporter *MRP4/ABCC4* is a marker of poor prognosis in neuroblastoma and confers resistance to irinotecan in vitro. Mol. Cancer Ther. **4:** 547–553.

Nowell, P. C., L. Jackson, A. Weiss, and R. Kurzrock, 1988 Historical communication: Philadelphia-positive chronic myelogenous leukemia followed for 27 years. Cancer Genet. Cytogenet. **34:** 57–61.

Oka, A., H. Sugisaki and M. Takanami, 1981 Nucleotide sequence of the kanamycin resistance transposon Tn903. J. Mol. Biol. **147:** 217–226.

Ozcan, S., L. G. Vallier, J. S. Flick, M. Carlson and M. Johnston, 1997 Expression of the *SUC2* gene of *Saccharomyces cerevisiae* is induced by low levels of glucose. Yeast **13:** 127–137.

Pedersen, B., J. M. Norgaard, B. B. Pedersen, N. Clausen, I. H. Rasmussen *et al.*, 2000 Many unbalanced translocations show

duplication of a translocation participant. Clinical and cytogenetic implications in myeloid hematologic malignancies. Am. J. Hematol. **64:** 161–169.

Perez-Ortin, J. E., A. Querol, S. Puig and E. Barrio, 2002 Molecular characterization of a chromosomal rearrangement involved in the adaptive evolution of yeast strains. Genome Res. **12:** 1533–1539.

Perlman, D., H. O. Halvorson and L. E. Cannon, 1982 Presecretory and cytoplasmic invertase polypeptides encoded by distinct mRNAs derived from the same structural gene differ by a signal sequence. Proc. Natl. Acad. Sci. USA **79:** 781–785.

Polakova, S., C. Blume, J. A. Zarate, M. Mentel, D. Jorck-Ramberg *et al.*, 2009 Formation of new chromosomes as a virulence mechanism in yeast *Candida glabrata*. Proc. Natl. Acad. Sci. USA **106:** 2688–2693.

Putnam, C. D., T. K. Hayes and R. D. Kolodner, 2009 Specific pathways prevent duplication-mediated genome rearrangements. Nature **460:** 984–989.

Rowley, J. D., 2001 Chromosome translocations: dangerous liaisons revisited. Nat. Rev. Cancer **1:** 245–250.

Rowley, J. D., 2008 Chromosomal translocations: revisited yet again. Blood **112:** 2183–2189.

Sambrook, J., E. F. Fritsch and T. Maniatis, 1989 *Molecular Cloning: A Laboratory Manual*. Cold Spring Harbor Laboratory Press, Cold Spring Harbor, NY.

Svetec, I. K., A. Stafa and Z. Zgaga, 2007 Genetic side effects accompanying gene targeting in yeast: the influence of short heterologous termini. Yeast **24:** 637–652.

Taki, T., and M. Taniwaki, 2006 Chromosomal translocations in cancer and their relevance for therapy. Curr. Opin. Oncol. **18:** 62–68.

Taussig, R., and M. Carlson, 1983 Nucleotide sequence of the yeast *SUC2* gene for invertase. Nucleic Acids Res. **11:** 1943–1954.

Torres, E. M., T. Sokolsky, C. M. Tucker, L. Y. Chan, M. Boselli *et al.*, 2007 Effects of aneuploidy on cellular physiology and cell division in haploid yeast. Science **317:** 916–924.

Tosato, V., S. K. Waghmare and C. V. Bruschi, 2005 Non-reciprocal chromosomal bridge-induced translocation (BIT) by targeted DNA integration in yeast. Chromosoma **114:** 15–27.

Tosato, V., C. Nicolini and C. V. Bruschi, 2009 DNA bridging of yeast chromosomes VIII leads to near-reciprocal translocation and loss of heterozygosity with minor cellular defects. Chromosoma **118:** 179–191.

VanHulle, K., F. J. Lemoine, V. Narayanan, B. Downing, K. Hull *et al.*, 2007 Inverted DNA repeats channel repair of distant double-strand breaks into chromatid fusions and chromosomal rearrangements. Mol. Cell. Biol. **27:** 2601–2614.

Wach, A., A. Brachat, R. Pohlmann and P. Philippsen, 1994 New heterologous modules for classical or PCR-based gene disruptions in *Saccharomyces cerevisiae*. Yeast **10:** 1793–1808.

Waghmare, S. K., and C. V. Bruschi, 2005 Differential chromosome control of ploidy in the yeast *Saccharomyces cerevisiae*. Yeast **22:** 625–639.

Waghmare, S. K., V. Caputo, S. Radovic and C. V. Bruschi, 2003 Specific targeted integration of kanamycin resistance-associated nonselectable DNA in the genome of the yeast *Saccharomyces cerevisiae*. Biotechniques **34:** 1024–1028, 1033.

Weinstock, D. M., C. A. Richardson, B. Elliott and M. Jasin, 2006 Modeling oncogenic translocations: distinct roles for double-strand break repair pathways in translocation formation in mammalian cells. DNA Repair (Amst.) **5:** 1065–1074.

Communicating editor: N. M. Hollingsworth

GENETICS

Supporting Information
http://www.genetics.org/cgi/content/full/genetics.110.120683/DC1

Different Aneuploidies Arise From the Same Bridge-Induced Chromosomal Translocation Event in *Saccharomyces cerevisiae*

Beatrice Rossi, Pawan Noel and Carlo V. Bruschi

DOI: 10.1534/genetics.110.120683

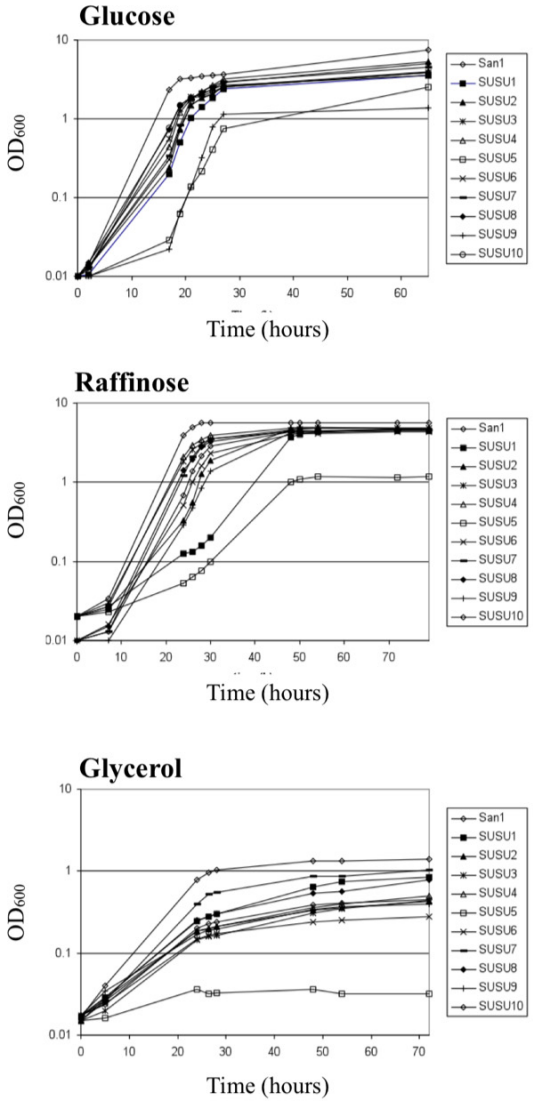

FIGURE S1.—Growth test in different carbon sources. The control strain San1 and all the 10 SUSU translocants were cultured in YPD medium and OD_{600} was measured at identical times.

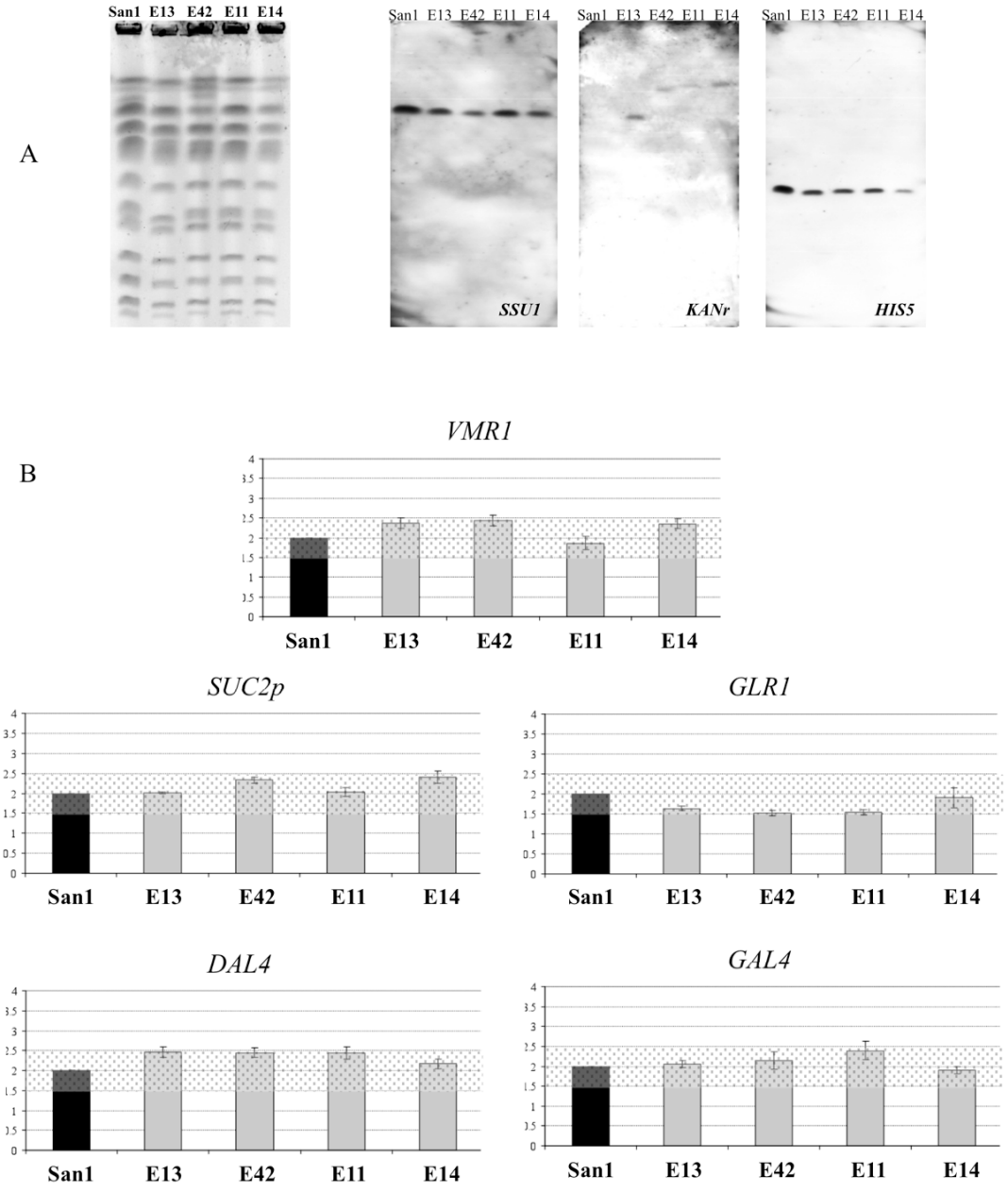

FIGURE S2.—Genomic characterization of *KANMX4* ectopic integrants. A) Chromosome separation by CHEF and Southern blot analysis performed using SSU1 probe on Chr. XVI, HIS5 on Chr. IX and KANMX4 showing ectopic integration. San1, control strain. E13 and E42 are two ectopic clones obtained by LiAC transformation while E11 and E14 were obtained by spheroplast transformation. B) Gene copy number determination of genes located on Chr. XVI and Chr. IX showing that no variation in the diploid chromosome condition is present in the ectopic strains. The gene dosage of *VMR1*, located on chromosome VIII, but not involved in translocation, was also determined as control for the accuracy of our experiments. Each analyzed gene and *ACT1* were co-amplified in the same PCR reaction and data were normalized as described in Figure 3.

San1: parental strain; E13, E42, E11 and E14, ectopic clones.
For other symbols and explanations see Figure 3.

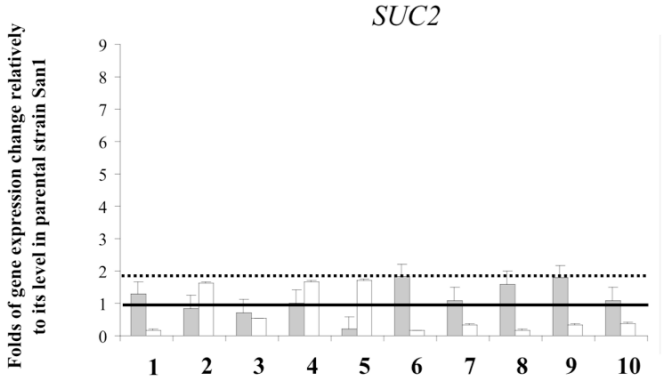

FIGURE S3.—Gene expression analyses of *SUC2* on glucose and raffinose. The graph reports the expression levels of *SUC2* on glucose (grey bars) and on raffinose (white bars). The expression level of *SUC2* was normalized with the expression level of the control gene *HSC82* and then compared with the normalized expression of *SUC2* in the San1 control strain considered as unit (horizontal black line). Dotted black line, two fold increase in gene expression relatively to the expression level in parental strain.

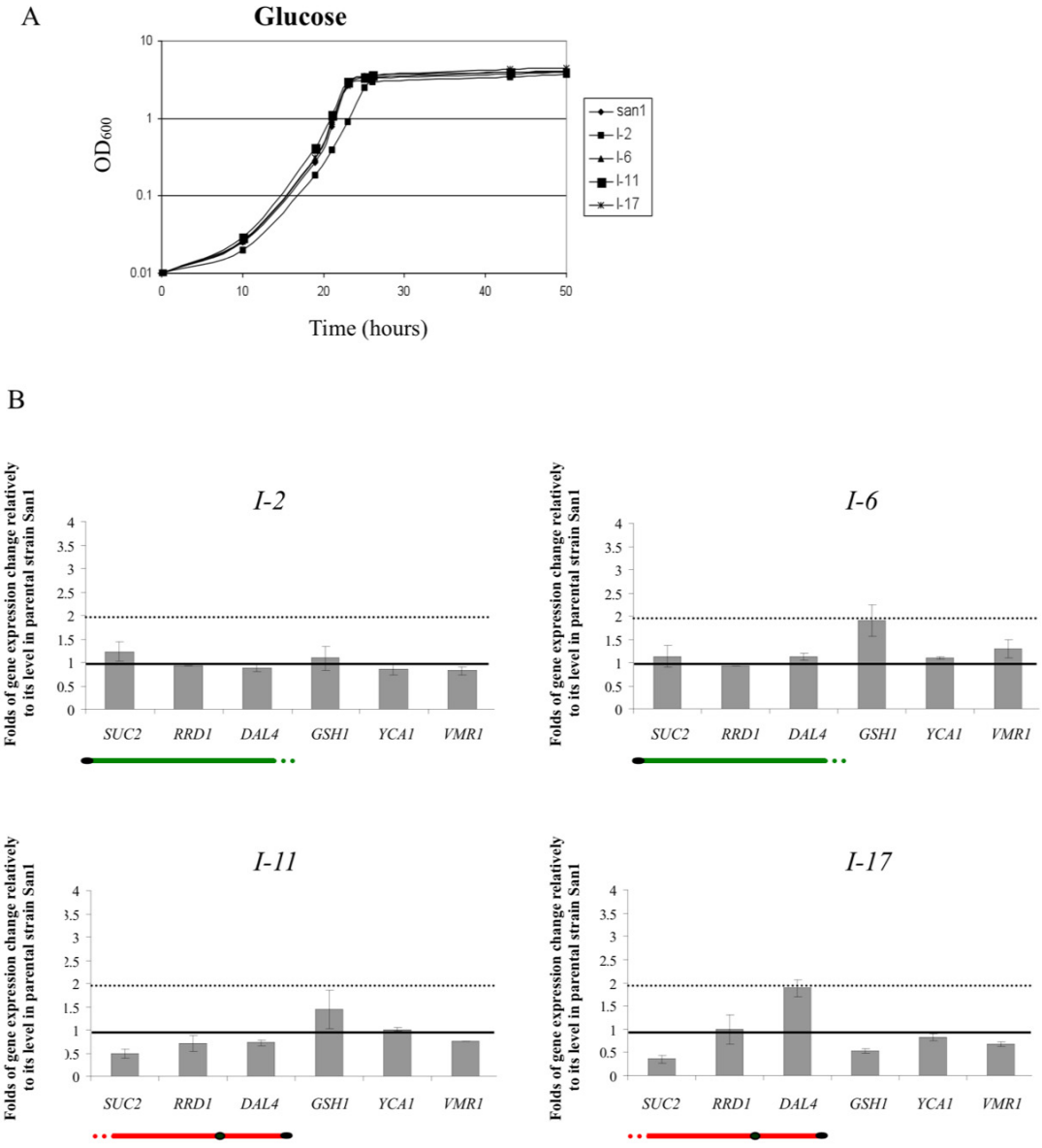

FIGURE S4.—Characterization of strains carrying *KANMX4* integration on either translocation break points on chromosomes XVI and IX. A) Growth test in glucose showing wild type-like growth of all the strains. Experimental conditions are described in Figure S1. B) Gene expression analyses of chromosome XVI specific genes in I-2 and I-6 and chromosome IX specific genes in I-11 and I-17. *GSH1*, *YCA1* and *VMR1* expression was analyzed for all four *KANMX4* integrants. For calculations and methods refer to Figure 8. The relative positions of the genes on both chromosomes is schematically represented under each histogram.

TABLE S1A

Oligonucleotides used as PCR primers in this work

Name	Nucleotide sequence	Use
Fw(XVI)	5` TCTCAGTATATTTTGCTGCTTTCCTTCATATGTATATATATCTATT TACATATTAGTTTACAGAAGTCGACGGATCCCCGGGTTAA 3`	Amplification of integration and BIT cassette (c.)
Rev(IX)	5`CTTTGCTGGGGGAGCGAGAACTACGCTAGGACAACAACTCCCATACGGTAAATGTCTTAGTATGTCCGCGCGTTGGCCGATTCAT 3`	Amplification of integration and BIT cassette (c.)
(IX)ins-fw	5`AAGGACAGGGGCACGGTGAGCTGTCGAAGGTATCCATTTTATCATGTTTC GTTTGTACAAGCACGGTCGACGGATCCCCGGGTTAA3`	Amplification of integration cassette
(XVI)ins-rev	5`TGTTCGTGGACATAGTTCTTATCTGTAGACTTCTAAATGTTTGTTTGGTTGCAGAAAGCATAAAGCCGCGCGTTGGCCGATTCAT 3`	Amplification of integration cassette
ssu1Fw	-5` CGGAGCTTTCCATTTGGAAT 3`-	BIT c. integration
ssu1Rev	-5` CGATGACGAGGTAATCGTAA 3`-	BIT c. integration
SUC2FwNEW	-5` ATAGGGGCTTAGCATCCACA 3`-	BIT c. integration
SUC2RevNEW	-5` CCTGGACGTGGGGTCGATTA 3`-	BIT c. integration
K1	-5` ACAATCGATAGATTGTCGCAC 3`-	BIT c. integration
K2	-5` TCAGTCGTCACTCATGGTGAT 3`-	BIT c. integration
SSU1RTfw	-5` TGGTATGATCTCGCAGTCTGTCTAG 3`-	RT-PCR of *SSU1*
SSU1RTrev	-5`AAAGGCATAGAATTGACCAACAAA 3`-	RT-PCR of *SSU1*
SUC2RTfw	-5` GATCCTTCCAAATCTTATTGGGTC 3`-	RT-PCR of *SUC2*
SUC2RTrev	-5`CATGTTCACAGATCCTAGAGCGTTA 3`-	RT-PCR of *SUC2*
GLR1fw	-5` TCTGATGGGTTCTTTAGATTGGAAG 3`-	RT-PCR of *GLR1*
GLR1rev	-5` AGTAACCAATTCTTCTGCGCTAGTC 3`-	RT-PCR of *GLR1*
GSH1fw	-5` GCCAAAGACGTACAAGATAAAGTCC 3`-	RT-PCR of *GSH1*
GSH1rev	-5` TTTCAGCTCCTAAAAAGGATGTCAA 3`-	RT-PCR of *GSH1*
CLB1_For	-5` TAGAGCAGGATGACCAGAAAAAGTT 3`-	RT-PCR of *CLB1*
CLB1_Rev	-5` TCGTCGTGAATAGTAGATCCAACAA 3`-	RT-PCR of *CLB1*
VMR1Fw	-5` TTACTATCATCCCTCAGGAC 3`-	RT-PCR of *VMR1*
VMR1Rev	-5` TTGCTTCAAAAGCTCTAGGC 3`-	RT-PCR of *VMR1*
CdcFw	-5` CCCAGTCTTACATCCAGACCAATAC 3`-	RT-PCR of *CDC48*
CdcRev	-5` GATGCTTTCATTTGCTGTGAGTATG 3`-	RT-PCR of *CDC48*
YCFw	-5` TCCACCTCAAACACAAACTATCAA 3`-	RT-PCR of *YCA1*
YCRev	-5` TACTTACCAGCCAATTCTTTCCTCA 3`-	RT-PCR of *YCA1*
CAR1fw	-5` GGAAAGTTGAAAATGGAGAAGGACT 3`-	RT-PCR of *CAR1*
CAR1rev	-5` TACAATAAGGTTTCACCCAATGCAC 3`-	RT-PCR of *CAR1*
MUC1Fw	-5` ATTCCAACCACTTACCTAACCACAA 3`-	RT-PCR of *MUC1*
MUC1Rev	-5` TTCCAAGAACCTTGATATTAGCAGC 3`-	RT-PCR of *MUC1*

TABLE S1B

Oligonucleotides used as PCR primers in this work

Name	Nucleotide sequence	Use
RRD1Fw	-5` CCAGGTCCTAGAAGGTATGGTAACC 3`-	RT-PCR of *RRD1*
RRD1Rev	-5` CGACTGGTTTTGATGGCTTAGTAAA 3`-	RT-PCR of *RRD1*
GAL4fw	-5` CCTCGAGAAGACCTTGACAT 3`-	RT-PCR of *GAL4*
GAL4rev	-5` ATGGTCGGGAGCCTGTTAAC 3`-	RT-PCR of *GAL4*
DAL4fw	-5`CAGAGACTTGAAACCGGTTG 3`-	RT-PCR of *DAL4*
DAL4rev	-5` GCATACCATACTATAGCCAT 3`-	RT-PCR of *DAL4*
Hsc 82 For	-5` TACATGAGGACACTCAAAACAGAGC 3`-	RT-PCR of *HDC82*
Hsc 82 Rev	-5` TAATCAACTTCTTCCATCTCGGTGT 3`-	RT-PCR of *HSC82*
act1FW	-5` TGAAGCTCAATCCAAGAGAGGTATC 3`-	Gene copy number control
ACT1Rev	-5` TTTGTTGGAAGGTAGTCAAAGAAGC 3`-	Gene copy number control
SouthSSU1FW	-5` ATCGATGACGTTGACGAATT 3`-	Gene copy number of *GLR1*
SouthSSU1REV	-5` GAGGAATCACCAACAATGTG 3`-	Gene copy number of *GLR1*
SouthSUC2FW	-5` TACTAACATGGCAGCATGC 3`-	Gene copy number of *SUC2p*
SouthSUC2REV	-5` CGACGGCATTAGCAAAGCTT 3`-	Gene copy number of *SUC2p*
Kanfw	-5` GGTGCGACAATCTATCGACGA 3`-	Amplification CHEF probe
Kanrev	-5` AGAAATCACCATGAGTGACGA 3`-	Amplification CHEF probe
KANnewFW	-5` ATTGATGTTGGACGAGTCGG 3`-	Gene copy number of *KANMX4*
KANnewREV	-5` ACGACTCACTATAGGGAGAC 3`-	Gene copy number *KANMX4*
SDL1fw	-5` AATGACTTACTATGAAAAGA 3`-	Amplification CHEF probe
SDL1rev	-5` TCGTGCCTCAAGTATTCCATC 3`-	Amplification CHEF probe
GLN1fw	-5` GGTAGAACTTTGAAGAAGAG 3`-	Gene copy number of *GLN1*
GLN1rev	-5` TGGCCATCCGTAAACATCGT 3`-	Gene copy number of *GLN1*
HIS5fw	-5` TTAGAGCATGCTGTGTTCCC 3`-	Amplification CHEF probe
HIS5rev	-5` ACTCTGCTGTTGCATATGTC 3`-	Amplification CHEF probe
CFD1Fw	-5` AACAGGAGATAGGCGTTCCT 3`-	Amplification CHEF probe
CFD1Rev	-5` GGAATATCTCAGCTCCTCTG 3`-	Amplification CHEF probe
PEP4fw	-5` TCACTGAAGGTGGTCACGAT 3`-	Amplification CHEF probe
PEP4rev	-5` CCATCGAACTTGCCAAATGC 3`-	Amplification CHEF probe

TABLE S1C

Oligonucleotides used as PCR primers in this work

Name	Nucleotide sequence	Use
DFDBP1	-5 ATGGCAGACTTGCCACAG9AAGGTATCTAATTTAAGCATCAAAA AATAGGCGTATCACGAG 3`-	Amplification of deletion cassette
RKANDBP1	-5 AAGGAGTTCTATATTTGGATTAGTCTTTTATTCTTTCTGCTCGATG ATAAGGTGTGAAAG 3`	Amplification of deletion cassette
GUT2DFw	-5 GCCACAAATAGGGAACTTTGGTCTAAAGCAAGGACTCTCCGTCG ACGGATCCCCGGGTTAA 3`-	Amplification of deletion cassette
GUT2DrevNEW	-5` CCATTAAGGAAAATAGGTAATAATAGCGATTTCATTGCCATCCG CGCGTTGGCCGATTCAT 3`-	Amplification of deletion cassette
DBP1 F1	-5` CGTAAATATTACCCCGCGAG 3`-	Deletion analysis
DBP1 R2	-5` CACCCATTTATGATTGGGAC 3`-	Deletion analysis
DBP1 F2	-5` AGAACTAGGGGAGGAGGAGG 3`-	Deletion analysis
DBP1 R1	-5` TTCGCGTTCTTAGGCCCCGG 3`-	Deletion analysis
gut2CONTFw2	-5` GGAACCCGTTCCTCTATCAT 3`-	Deletion analysis
gut2CONTFw2	-5` GGAACCCGTTCCTCTATCAT 3`-	Deletion analysis
GUT2contREV1	-5` ACCCCACCGTGAATCATCTT 3`-	Deletion analysis
GUT2contDFw	-5` AGCACGTCATGCACCTGTTT 3`-	Deletion analysis
GUT2contRev	-5` AGGTTGTCAAGGCAGATAGG 3`-	Deletion analysis

TABLE S2

Number of integration events obtained using LiAc and spheroplast transformation.

Site of integration	LiAC transformation	Spheroplast transformation
SUC2 (Chr. IX)	55	38
SSU1 (Chr. XVI)	1	2
Ectopic	39	87
Translocant SSU1 – SUC2	9	1
Total	**104**	**138**

TABLE S3

Names, location and short description of the functions of the genes analyzed by RT-PCR.

Name of the gene	Chromosome location	Function
GAL4	Ch. XVI	DNA-binding transcription factor required for the activation of the GAL genes in response to galactose.
CAR1	Ch. XVI	Arginase, responsible for arginine degradation.
SSU1	Ch. XVI- T.B.P	Plasma membrane sulfite pump involved in sulfite metabolism and required for efficient sulfite efflux.
SUC2	Ch. IX- T.B.P	Invertase, sucrose hydrolyzing enzyme; a secreted, glycosylated form is regulated by glucose repression, and an intracellular, nonglycosylated enzyme is produced constitutively.
RRD1	Ch. IX	Peptidyl-prolyl cis/trans-isomerase, activator of the phosphotyrosyl phosphatase activity of PP2A; involved in G1 phase progression, microtubule dynamics, bud morphogenesis and DNA repair.
MUC1	Ch. IX	GPI-anchored cell surface glycoprotein (flocculin) required for pseudohyphal formation, invasive growth, flocculation, and biofilms.
DAL4	Ch. IX	Allantoin permease
GLR1	Ch. XVI – T.B.P.	Cytosolic and mitochondrial glutathione oxidoreductase, converts oxidized glutathione to reduced glutathione.
GSH1	Ch. X	Gamma glutamylcysteine synthetase catalyzes the first step in glutathione (GSH) biosynthesis.
YCA1	Ch. XV	Putative cysteine protease similar to mammalian caspases; involved in regulation of apoptosis upon hydrogen peroxide treatment.
CDC48	Ch. IV	ATPase in ER, nuclear membrane and cytosol with homology to mammalian p97; in a complex with Npl4p and Ufd1p participates in retrotranslocation of ubiquitinated proteins from the ER into the cytosol for degradation by the proteasome.
CLB1	Ch. VII	B-type cyclin that activates Cdc28p to promote the transition from G2 to M phase of the cell cycle.
VMR1	Ch. VIII	Vacuolar multidrug resistance protein member of the ATP-binding cassette (ABC) family.